1 **Impact of air pollution control measures and regional transport on**

2 **carbonaceous aerosols in fine particulate matter in urban Beijing,**

3 **China: Insights gained from long-term measurement**

4 Dongsheng Ji[1, 2*], Wenkang Gao[1, 2], Willy Maenhaut[3*], Jun He[4], Zhe Wang[1, 5], Jiwei Li[1, 6], Wupeng

5 Du[7], Lili Wang[1, 2], Yang Sun[1, 2], Jinyuan Xin[1, 2], Bo Hu[1, 2], Yuesi Wang[1, 2*]

6 *[1] State Key Laboratory of Atmospheric Boundary Layer Physics and Atmospheric Chemistry,*

7 *Institute of Atmospheric Physics, Chinese Academy of Sciences, Beijing, 100191, China*

8 *[2] Atmosphere Sub-Center of Chinese Ecosystem Research Network, Institute of Atmospheric Physics,*

9 *Chinese Academy of Sciences, Beijing, 100191, China*

10 *[3] Department of Chemistry, Ghent University, Gent, 9000, Belgium*

11 *[4] Natural Resources and Environment Research Group, International Doctoral Innovation Centre,*

12 *Department of Chemical and Environmental Engineering, University of Nottingham Ningbo China,*

13 *Ningbo, 315100, China*

14 *[5] Research Institute for Applied Mechanics, Kyushu University, Fukuoka, 816-8580, Japan*

15 *[6] University of Chinese Academy of Sciences, Beijing, 100049, China*

16 *[7] Institute of Urban Meteorology, Chinese Academy of Meteorological Sciences, Beijing, 100081,*

17 *China*

18

19 Correspondence to: Dongsheng Ji (jds@mail.iap.ac.cn), Willy Maenhaut (Willy.Maenhaut@UGent.be)

20 and Yuesi Wang (wys@dq.cern.ac.cn)

21

Abstract As major chemical components of airborne fine particulate matter ($PM_{2.5}$), organic carbon (OC) and elemental carbon (EC) have vital impacts on air quality, climate change, and human health. Because OC and EC are closely associated with fuel combustion, it is helpful for the scientific community and policymakers assessing the efficacy of air pollution control measures to study on the impact of the control measures and regional transport on the OC and EC levels. In this study, hourly mass concentrations of OC and EC associated with $PM_{2.5}$ were semi-continuously measured from March 2013 to February 2018. The results showed that annual mean OC and EC concentrations declined from 14.0 to 7.7 $\mu g/m^3$ and from 4.0 to 2.6 $\mu g/m^3$, respectively, from March 2013 to February 2018. In combination with the data of OC and EC in previous studies, an obvious decreasing trend in OC and EC concentrations was found, which was caused by clean energy policies and effective air pollution control measures. However, no obvious change in the ratios of OC and EC to the $PM_{2.5}$ mass (on average, 0.164 and 0.049, respectively) was recorded, suggesting that inorganic ions still contributed a lot to $PM_{2.5}$. Based on the seasonal variations of OC and EC, it appeared that higher OC and EC concentrations were still observed in the winter months, with the exception of winter of 2017-2018. Traffic policies executed in Beijing resulted in nighttime peaks of OC and EC, caused by heavy-duty vehicles and heavy-duty diesel vehicles being permitted to operate from 0:00 to 6:00. In addition, the fact that there was no traffic restriction in weekends led to higher concentrations in weekends compared to weekdays. Significant correlations between OC and EC were observed throughout the study period, suggesting that OC and EC originated from common emission sources, such as exhaust of vehicles and fuel combustion. OC and EC levels increased with enhanced SO_2, CO and NO_x concentrations while the O_3 and OC levels enhanced simultaneously when O_3 concentrations were higher than 50 $\mu g/m^3$. Nonparametric wind regression analysis was performed to examine the sources of OC and EC in the Beijing area. It was found that there were distinct hot spots in the northeast wind sector at wind speeds of approximately 5 km/h, as well as diffuse signals in the southwestern wind sectors. Source areas further away from Beijing were assessed by potential source contribution function (PSCF) analysis. A high-potential source area was precisely pinpointed, which was located in the northwestern and southern areas of Beijing in 2017 instead of solely in the southern areas of Beijing in 2013. This work shows that improvement of the air quality in Beijing benefits from strict control measures; however, joint prevention and

51   control of regional air pollution in the regions is needed for further improving the air quality. The

52   results provide a reference for controlling air pollution caused by rapid economic development in

53   developing countries.

54

55   **Key words** air pollution control measures, regional transport, organic carbon, elemental carbon,
56   Beijing

57

1 Introduction

Worldwide attention on atmospheric organic carbon (OC) and elemental carbon (EC) has been paid by the public and the scientific community because OC and EC have vital effects on air quality, atmospheric visibility, climate, and human health (Bond et al., 2013; Boucher et al., 2013; World Health Organization (WHO), 2012). OC is composed of thousands of organic compounds and occupies 10-50 % of the ambient $PM_{2.5}$ mass (Seinfeld and Pandis, 1998) while EC, which is emitted from fuel combustion, represents 1-13 % of the ambient $PM_{2.5}$ mass (Shah et al., 1986; Tao et al., 2017; Malm et al., 1994). Considering that OC and EC occupy high fractions of the $PM_{2.5}$, a decline in OC and EC concentrations will improve air quality. Due to the light scattering potential of OC and the light absorption ability of EC, high concentrations of OC and EC can impair the atmospheric visibility. In addition, OC and EC can affect the atmospheric energy balance through scattering and absorbing incoming and outgoing solar and terrestrial radiation (direct effect) and through modifying the microphysical properties of clouds, like influencing cloud condensation nuclei and/or ice nuclei (indirect effects). Direct and indirect effects of OC and EC remain one of the principal uncertainties in estimates of anthropogenic radiative forcing (Boucher et al., 2013). In particular, black carbon (BC also called EC) coated with secondary particles can enhance aerosol radiative forcing (Wang et al., 2013; Zhang et al., 2008). BC is found to aggravate haze pollution in megacities (Ding et al., 2016; Zhang et al., 2018). Most of all, OC and EC adversely affect human health. As important constituents of OC, polycyclic aromatic hydrocarbons (PAHs) are well known as carcinogens, mutagens, and teratogens and therefore pose a serious threat to the health and the well-being of humans (Boström et al., 2002). Short-term epidemiological studies provide sufficient evidence of all-cause and cardiovascular mortality and cardiopulmonary hospital admissions associated with daily variations in BC concentrations; besides, cohort studies proved that all-cause and cardiopulmonary mortality are linked with long-term average BC exposure (WHO, 2012). Thus, long-term continuous observations of OC and EC are a prerequisite to further study air quality, atmospheric visibility, climate effects, and human health. However, long-term continuous observations of OC and EC in China are scarce.

In the world, China is considered as one of the regions of high emissions of OC and EC due to high energy consumption and increasing vehicle population, accompanying rapid economic

development and urbanization for decades (http://www.stats.gov.cn/tjsj/ndsj/2017/indexch.htm). As the capital of China, Beijing with a residential population of 21.7 million, domestic tourists of 2.9×10^2 million and foreign tourists of approximately 3.3 million in 2017 (http://tjj.beijing.gov.cn/English/AD/) faces severe air pollution problems, which have attracted worldwide attention. A series of studies on OC and EC have already been performed in Beijing. Lang et al. (2017) indicated that OC showed a downward trend and EC had almost no change before 2003, both increased from 2003 to 2007, but decreased after 2007. The decline in OC concentrations was associated with coal combustion and motor vehicle emission control measures, while that in EC was caused by the replacement of fossil fuel and control of biomass emissions. Tao et al. (2017) stated that the nearly 30 % reduction in total carbon (TC) in recent years in Beijing can be taken as a real trend. Lv et al. (2016) found that the concentrations of OC and EC remained unchanged from 2000 to 2010 in Beijing. Yang et al. (2011a) conducted a long-term study of carbonaceous aerosol from 2005 to 2008 in urban Beijing and found a decline in the ratio of carbonaceous species to the $PM_{2.5}$ mass in contrast to what was observed 10 years earlier, which indicated that the importance of carbonaceous species in $PM_{2.5}$ had decreased. In addition, pronounced seasonal variations were recorded with the highest concentrations occurring in winter and the lowest ones in summer. Overall, these previous researches seem somewhat inconsistent with each other and they seldom focused on studying the impact of air pollution control measures and regional transport on the carbonaceous aerosol levels in detail.

Notably, a series of the strictest measures on emission abatement and pollution control were implemented in China from September 2013 (Jin et al., 2016). Substantial manpower and material resources have been put into improving the air quality in the past five years and significant measures are being taken for the atmospheric environment and ecosystem (Gao et al., 2017). To evaluate the effectiveness of air pollution control measures, it is necessary to conduct a long-term continuous observation of OC and EC and to study their long-term variation. Most of the previous studies showed average information for certain periods based on filter sampling and laboratory analysis and did not reflect the dynamic evolution processes of OC and EC with hourly resolution, which can provide important and detailed information for the potential health risk in the area with frequent occurrence of air pollution episodes. In addition, long-term measurements in urban areas of China

116 with high population density were scarce (Yang et al., 2005, 2011a; Zhang et al., 2011; Li et al.,

117 2015; Chang et al., 2017) and the knowledge on long-term continuous hourly observations is still

118 lacking, which is yet important for recognizing the influence of source emissions on air quality.

119   Based on the-above mentioned background, it is necessary to perform a long-term continuous

120 hourly observation to explore the characteristics of OC and EC, to examine the relationship between

121 OC and EC and with major air pollutants and their sources so as to better assess the influence of

122 emission control measures on the OC and EC levels. In this study, inter-annual, seasonal, weekly

123 and diurnal variation of OC and EC were investigated. The influence of local and regional

124 anthropogenic sources was evaluated using non-parametric wind regression (NWR) and potential

125 contribution source function (PSCF) methods. This study will be helpful for improving the

126 understanding of the variation and sources of OC and EC associated with $PM_{2.5}$ and assessing the

127 effectiveness of local and national PM control measures and it provides a valuable dataset for

128 atmospheric modelling study and assessing the health risk. It also is the first time that a continuous

129 hourly measurement for a 5-year period based on the thermal-optical method is reported for urban

130 Beijing.

131 **2 Experimental**

132 **2.1 Description of the site**

133   The study site (39°58'28'' N, 116°22'16'' E, 44 m above ground) was set up in the second floor

134 in the campus of the State key laboratory of atmospheric boundary physics and atmospheric

135 chemistry of the Institute of atmospheric Physics, Chinese Academy of Science (Fig. 1). The site is

136 approximately 1 km south from the 3rd Ring Road (main road), 1.2 km north from the 4th Ring

137 Road (main road), 200 m west of the G6 Highway (which runs north-south) and 50 m south of the

138 Beitucheng West Road (which runs east-west), respectively. The annual average vehicular speeds in

139 the morning and evening traffic peaks were approximately 27.8 and 24.6 km/h, respectively, in the

140 past five years. During the whole study period the level of traffic congestion is mild based on the

141 traffic performance index published by the Beijing Traffic Management Bureau

142 (http://www.bjtrc.org.cn/), which indicated 1.5-1.8 times more time will be taken to publicly travel

143 during traffic peaks than during smooth traffic. The study site is surrounded by residential zones, a

144 street park and a building of ancient relics without industrial sources. The experimental campaign

145 was performed from March 1, 2013 to February 28, 2018. The periods of March 1, 2013 to February

146 28, 2014, March 1, 2014 to February 28, 2015, March 1, 2015 to February 28, 2016, March 1, 2016

147 to February 28, 2017 and March 1, 2017 to February 28, 2018 are, hereinafter, called for short 2013,

148 2014, 2015, 2016 and 2017, respectively.

149 **2.2 Instrumentation**

150 Concentrations of $PM_{2.5}$-associated OC and EC were hourly measured with semi-continuous

151 thermal-optical transmittance method OC/EC analyzers (Model 4, Sunset Laboratory Inc. Oregon,

152 Unite states of America (USA)). The operation and maintenance are strictly executed according to

153 standard operating procedures (SOP, https://www3.epa.gov/ttnamti1/spesunset.html). Volatile

154 organic gases are removed by an inline parallel carbon denuder installed upstream of the analyzer.

155 A round 16-mm quartz filter is used to collect $PM_{2.5}$ with a sampling flow rate of 8 L/m. A modified

156 NIOSH thermal protocol (RT-Quartz) is used to measure OC and EC. The sampling period is 30

157 min and the analysis process lasts for 15 min. Calibration is performed according to the SOP. An

158 internal standard CH_4 mixture (5.0 %; ultra-high purity He) is automatically injected to calibrate the

159 analyzer at the end of every analysis. In addition, off-line calibration was conducted with an external

160 amount of sucrose standard (1.06 μg) every three months. The quartz fiber filters used for sample

161 collection were replaced by new ones before the laser correction factor dropped below 0.90. After

162 replacement, a blank measurement of the quartz fiber filters is carried out. The uncertainty of the

163 TC measurement has been estimated to be approximately ±20 % (Peltier et al., 2007). The

164 analyzers/monitors for O_3, CO, SO_2, NO_x and $PM_{2.5}$, and their precision, detection limits and

165 calibration methods have been described in detail elsewhere (Ji et al., 2014). Briefly, O_3 was

166 measured using an ultraviolet photometric analyzer (model 49i, Thermo Fisher Scientific (Thermo),

167 USA), CO with a gas filter correlation nondispersive infrared method analyzer (model 48i, Thermo,

168 USA), SO_2 using a pulsed-fluorescence analyzer (model 43i, Thermo, USA), $NO-NO_2-NO_x$ with a

169 chemiluminescence analyzer (model 42, Thermo, USA) and $PM_{2.5}$ using a US Environmental

170 Protection Agency Federal Equivalent Method analyzer of $PM_{2.5}$ (SHARP 5030, Thermo, USA).

171 Meteorological data such as wind speed (WS), wind direction (WD), relative humidity (RH) and

172 atmospheric temperature (T) were recorded via an automatic meteorological station (Model

173 AWS310; Vaisala, Finland). The data were processed using an Igor-based software (Wu et al., 2018)

174 and the commercial software of Origin.

175 **2.3 NWR and PSCF methods**

176 **2.3.1 NWR method**

177 NWR is a source-to-receptor source identification model, which provides a meaningful

178 allocation of local sources (Henry et al., 2009; Petit et al., 2017). Wind analysis results using NWR

179 were obtained using a new Igor-based tool, named ZeFir, which can perform a comprehensive

180 investigation of the geographical origins of the air pollutants (Petit et al., 2017). The principle of

181 NWR is to smooth the data over a fine grid so that concentrations of air pollutants of interest can be

182 estimated by any couple of wind direction (θ) and wind speed (u). The smoothing is based on a

183 weighing average where the weighing coefficients are determined using a weighting function $K(\theta,$

184 $u, \sigma, h) = K_1 (\theta, \sigma) \times K_2 (u, h)$ (i.e., Kernel functions). The estimated value (E) given θ and u is

185 calculated by the following equations (1)-(3):

186 $$E(\theta|u) = \frac{\sum_{i=1}^{N} K1\left(\frac{\theta - Wi}{\sigma}\right) \times K2\left(\frac{u - Yi}{h}\right) \times Ci}{\sum_{i=1}^{N} K1\left(\frac{\theta - Wi}{\sigma}\right) \times K2\left(\frac{u - Yi}{h}\right)} \qquad (1)$$

187 $$K_1(x) = \frac{1}{\sqrt{2\pi}} \times e^{-0.5x^2} \qquad -\infty < x < \infty \qquad (2)$$

188 $$K_2(x) = 0.75 \times (1 - x^2) \qquad -1 < x < 1 \qquad (3)$$

189 where σ and h were smoothing parameters, which can be suggested by clicking on the button of

190 suggest estimate in the software of Zefir; Ci, Wi, and Yi are the observed concentration of a pollutant

191 of interest, resultant wind speed and direction, respectively, for the ith observation in a time period

192 starting at time t_i; N is the total number of observations.

193 After the calculation, graphs of the estimated concentration and the joint probability are

194 generated. The NWR graph of the air pollutant of interest, acquired directly via the NWR calculation,

195 represents an integrated picture of the relationship of estimated concentration of the specific

196 pollutant, wind direction and wind speed. The graph of the joint probability for the wind data,

197 equivalent to a wind rose, shows the occurrence probability distribution of the wind speed and wind

198 direction.

199 **2.3.2 PSCF method**

200 The PSCF method is based on the residence time probability analysis of air pollutants of

201 interest (Ashbaugh et al., 1985). Source locations and preferred transport pathways can be identified

(Poirot and Wishinski, 1986; Polissar et al., 2001; Lupu and Maenhaut, 2002). The potential

locations of the emission sources are determined using backward trajectories. A detailed description

can be found in Wang et al. (2009). In principle, the PSCF is expressed using equation (4):

$$PSCF(i, j) = w_{ij} \times (m_{ij}/n_{ij}) \tag{4}$$

where w_{ij} is an empirical weight function proposed to reduce the uncertainty of n_{ij} during the study

period, m_{ij} is the total number of endpoints in (i, j) with concentration value at the receptor site

exceeding a specified threshold value (the 75th percentiles for OC and EC each year were used as

threshold values to calculate m_{ij}) and n_{ij} is the number of back-trajectory segment endpoints that fall

into the grid cell (i, j) over the period of study. The National Oceanic and Atmospheric

Administration Hybrid Single-Particle Lagrangian Integrated Trajectory model

(https://ready.arl.noaa.gov/HYSPLIT.php) was used for calculating the 48-h backward trajectories

terminating at the study site at a height of 100 m every 1 h from March 1 2013 to February 28 2018.

In this study, the domain for the PSCF was set in the range of (30-70 °N, 65-150 °E) with the grid

cell size of 0.25 × 0.25°.

3 Results and discussion

3.1 Levels of OC and EC

Statistics for the OC and EC concentrations from March 1, 2013 to February 28, 2018 are

summarized in Table 1. Benefiting from the Air Pollution Prevention and Control Action Plan and

increasing atmospheric self-purification capacity (ASC, shown in Table S1), a decline in annual

average concentrations is on the whole recorded. In detail, the annual average concentrations of both

OC and EC peaked in 2014 and then started to decline gradually during the remainder of the study

period. Nonetheless, the annual average concentrations of $PM_{2.5}$ were generally decreasing from

2013 to 2017. To assess whether the decreases are statistically significant, 2-tailed paired t-tests

were applied for OC, EC and $PM_{2.5}$ using their monthly average concentrations in 2013 and 2016

as paired datasets. At a confidence level of 98%, from March to October, the paired data are

statistically different, indicating that the concentrations of OC, EC and $PM_{2.5}$ declined during the

above period from 2013 to 2016; however, the concentrations of OC, EC and $PM_{2.5}$ during

November and February from 2013 to 2016 are not statistically different. The decline in OC and EC

concentrations is closely associated with decreasing coal consumption, increasing usage of natural

231   gases and the implementation of a stricter vehicular emission standard and increasing atmospheric

232   self-purification capacity (Tables S1-S3). Knowledge of the relative contribution of OC and EC to

233    $PM_{2.5}$ is important in formulating effective control measures for ambient PM (Wang et al., 2016a).

234   The ratios of OC and EC to $PM_{2.5}$ varied little during the whole study period, suggesting that

235   vehicular emission might be an important contributor of OC and EC although several other pollution

236   sources also contributed to the OC and EC loadings. The ratios of OC to $PM_{2.5}$ ranged from 15.5 to

237   17.8 % with the average of 16.4 %, while those of EC to $PM_{2.5}$ ranged from 4.5 to 5.2 % with the

238   average of 4.9 %. OC accounted, on average, for 77.0 ± 9.3 % of the total carbon (TC, the sum of

239   OC and EC), while EC amounted for 23.0 ± 9.3 % of the TC. These results are consistent with those

240   in previous studies (Wang et al., 2016a; Tao et al., 2017, Lang et al., 2017). The contribution of TC

241   to $PM_{2.5}$, 21.3 ± 15.8 %, is also similar to those reported in previous studies, listed in Table S4, for

242   example, at urban sites of Hongkong, China (23.5-23.6 % in 2013), Hasselt (23 %) and Mechelen

243   (24 %) in northern Belgium, rural sites in Europe (19-20 %) and some sites in India (on average,

244   20 %, Bisht et al., 2015; Ram and Sarin, 2010; Ram and Sarin, 2012), but lower than those observed

245   historically at multiple sites in China (on average 27 %, Wang et al., 2016a), with Beijing (27.6 %,

246   from March 2005 to Feb 2006), Chongqing (28.3 %, from March 2005 to February 2006), Shanghai

247   (34.5 %, from March 1999 to May 2000) and Guangzhou (26.4 %, December 2008 to February

248   2009), in Budapest (40 %), Istanbul (30 %), and many sites in the USA, like Fresno (43.2 %), Los

249   Angeles (36.9 %) and Philadelphia (33.3 %) (Na et al., 2004). Compared to previous studies in

250   Beijing (Table S4), the TC to $PM_{2.5}$ ratio became smaller in this study, indicating a relatively lower

251   contribution from carbonaceous aerosols to $PM_{2.5}$ in this study. The difference in the TC/$PM_{2.5}$ ratio

252   could be ascribed to two factors. One factor is the difference in characteristics of sampling locations

253   between that in our study and those in the earlier studies. However, our site and those in the previous

254   studies used for comparison are all located in urban areas of Beijing (Chaoyang and Haidian district,

255   respectively). It is reasonable to assume that they are affected by common sources since the

256   surrounding environments exhibit similar features. Besides, the annual average $PM_{2.5}$

257   concentrations in both districts published by the Ministry of Environmental Protection, China

258   (http://106.37.208.233:20035/) were quite comparable to each other from 2013 to 2017 ($y=0.99x$,

259    $r^2=0.92$), indicating that both areas had particle pollution of a similar degree. The other factor is that

260 the contribution from secondary inorganic ions to the $PM_{2.5}$ became more important because of a

261 stronger atmospheric oxidation capacity (the annual average O_3 concentrations were 102, 109, 116,

262 119, and 136 $\mu g/m^3$, respectively, from 2013 to 2017 in the Beijing-Tianjin-Hebei region; published

263 by http://106.37.208.233:20035/), which could give rise to a lower TC to $PM_{2.5}$ ratio. A higher TC

264 to $PM_{2.5}$ ratio suggests that there is a lower contribution from secondary inorganic ions to $PM_{2.5}$,

265 while a lower ratio may indicate a larger contribution from secondary inorganic ions to $PM_{2.5}$. The

266 carbonaceous aerosol (the sum of multiplying the measured OC by a factor of 1.4 and EC)

267 represented on average, 27.7 ± 16.7 % of the observed $PM_{2.5}$ concentration, making it a dominant

268 contributor to $PM_{2.5}$.

269 Table 3 lists recently published results for OC and EC mass concentrations in major megacities.

270 Although the observation periods were not same, a comparative analysis of OC and EC

271 concentrations between different megacities could show the status of energy consumption for

272 policymakers, drawing lessons and experience from other countries. It is obvious that the $PM_{2.5}$-

273 associated OC and EC levels in the megacities in the developing countries were far higher than

274 those in the developed countries. The $PM_{2.5}$-associated OC and EC concentrations in Beijing were

275 higher than those in Athens, Greece (2.1 and 0.54 $\mu g/m^3$), Los Angeles (2.88 and 0.56 $\mu g/m^3$) and

276 New York (2.88 and 0.63 $\mu g/m^3$), USA, Paris, France (3.0 and 1.4 $\mu g/m^3$), Soul, South Korea (4.1

277 and 1.6 $\mu g/m^3$), Tokyo, Japan (2.2 and 0.6 $\mu g/m^3$) and Toronto, Canada (3.39 and 0.5 $\mu g/m^3$). That

278 is because clean energy has widely been used and strict control measures are taken to improve the

279 air quality step by step in the developed countries. Of the megacities in the developing countries,

280 OC and EC concentrations in Beijing were lower than those in most other megacities, like Mumbai

281 and New Delhi, India, and Xi'an and Tianjin, China, but close to those in Shanghai and Hongkong,

282 China, and higher than those in Lhasa, China. These differences/similarities indicate that OC and

283 EC gradually declined in Beijing and that a series of measures had progressive effects. However, to

284 further improve the air quality, more synergetic air pollution abatement measures of carbonaceous

285 aerosols and volatile organic compounds (VOCs) emissions need to be performed.

286 Fig. 2 shows the mass fractions of carbonaceous aerosols in different $PM_{2.5}$ levels classified

287 according to $PM_{2.5}$ concentrations during the whole study period. There were 571, 561, 310, 169,

288 142 and 74 days for excellent, good, slightly polluted, moderately polluted, heavily polluted and

289 severely polluted air quality levels during the whole period. It was obvious that OC and EC

290 concentrations increased with the degradation of air quality. OC and EC concentrations were 6.3

291 and 1.7, 10.2 and 2.9, 13.7 and 4.1, 17.3 and 5.3, 24.6 and 7.9 and 35.5 and 11.3 $\mu g/m^3$ for excellent,

292 good, slightly polluted (LP), moderately polluted (MP), heavily polluted (HP) and severely polluted

293 (SP) air quality days, respectively (The criteria used to classify the air quality have been added in

294 the revised manuscript. Air quality as Excellent, good, LP, MP, HP and SP were based on the daily

295 average $PM_{2.5}$ concentration, i.e., excellent ($0 < PM_{2.5} \leqslant 35$ $\mu g/m^3$), good ($35 < PM_{2.5} \leqslant 75$ $\mu g/m^3$),

296 lightly polluted (LP, $75 < PM_{2.5} \leqslant 115$ $\mu g/m^3$), moderately polluted (MP, $115 < PM_{2.5} \leqslant 150$ $\mu g/m^3$),

297 heavily polluted (HP, $150 < PM_{2.5} \leqslant 250$ $\mu g/m^3$) and severely polluted (SP, $PM_{2.5} > 250$ $\mu g/m^3$),

298 respectively.). However, the percentages of OC and EC accounting to $PM_{2.5}$ decreased with the

299 deterioration of air quality. OC and EC made up for 31.5 % and 8.3 %, 18.9 % and 5.4 %, 14.7 %

300 and 4.4 %, 13.4 % and 4.1 %, 12.9 % and 4.2 % and 11.4 % and 3.6 % during excellent, good,

301 slightly polluted, moderately polluted, heavily polluted and severely polluted air quality days,

302 respectively. The percentage for OC decrease from 31.4 to 11.4 % while that for EC decreased from

303 8.3 to 3.6 % with the deterioration of air quality, indicating that other $PM_{2.5}$ constituents than OC

304 and EC contributed more to the increased $PM_{2.5}$ levels. This is consistent with previous studies

305 showing that secondary inorganic ions play a more important role in the increase in $PM_{2.5}$

306 concentrations (Ji et al., 2014, 2018).

307 **3.2 Inter-annual variation of OC and EC**

308 To evaluate the effect of the clean air act over a prolonged period, our OC and EC data were

309 combined with the data of previous studies for Beijing (He et al., 2011; Zhao et al., 2013; Ji et al.,

310 2016; Tao et al., 2017; Lang et al., 2017). As shown in Fig. 3, a decreasing trend in OC and EC

311 concentrations is on the whole observed. Table S2 summarizes a variety of policies and actions to

312 reduce pollutant emissions in power plants, coal-fired boilers, residential heating and traffic areas

313 in Beijing since 2002. Although the gross domestic product, population, energy consumption and

314 vehicular population rapidly increased (Table S3), the general decreasing trends in OC and EC

315 concentrations could be attributed to the combined effect of the more stringent traffic emission

316 standards and traffic restriction, the energy structure evolving from intensive coal and diesel

317 consumption to replacement with natural gas and electricity, and retrofitting with SO_2 and NO_2

12

318   removal facilities to meet the new emission standards applicable to different coal-fired facilities, etc.

319   In particular, there is an obvious dividing line of OC and EC concentrations in 2010. After 2010, the

320   OC and EC concentrations became substantially lower than those observed previously. In addition

321   to the measures mentioned in Table S2, the relocation of Shougang Corporation, which is one of the

322   China's largest steel companies, and other highly polluting factories out of Beijing might have

323   helped to some extent; all the small coal mines in Beijing were shut down and plenty of yellow label

324   (heavy-polluting) vehicles were forced off road. Note that the OC and EC levels in 2008 and 2009

325   were also somewhat lower, which was caused by a series of radical measures to improve the air

326   quality for the Olympic Games in 2008 and a decline in industrial production because of China's

327   exports crash in 2009, respectively. It suggests that a stringent clean air act and rectifying industry

328   played important roles in the air quality improvement.

329   In this study, the fire spots were counted in the domain of (30-70° N, 65-150° E) using the

330   MODIS Fire Information for Resource Management System (Giglio, 2013). Note also that the

331   effective control of biomass burning might contribute to the decrease in OC and EC concentrations.

332   In Fig. 3, it can be seen that the annual average EC concentration and fire spot counts exhibit a

333   rather similar variation from 2004 to 2017, except in the year 2012, which suggests that the EC

334   levels are somewhat correlated with the biomass burning; this might indicate that biomass burning

335   contributed somewhat to the EC levels. The reduction in fire spot counts from 2014 to 2017, which

336   resulted from efforts to control the agricultural field residue burning since 2013, helped to reduce

337   the EC concentrations to some extent, but the low EC levels during 2014-2017 are likely mostly due

338   to the implementation of the clean air act. With regard to the anomaly in the year 2012, based on

339   the MODIS data for this year, a very non-uniform distribution of fire spots in the BTH region was

340   observed, with a distinct decrease of fire spot counts in Beijing, but higher fire spot counts in the

341   southern Hebei Province; this may be ascribed to the fact that the policy of Banning Straw Burning

342   in Summer and Autumn was executed to different degrees in the whole region, with better

343   implementation in Beijing area and worse action in the other parts.

344   (http://www.beijing.gov.cn/zfxxgk/110029/qtwj22/2012-12/11/content_357114.shtml). In addition,

345   for the years from 2002 to 2017, the highest precipitation volume in Beijing was recorded in 2012,

346   i.e., 733.2 mm, and the rainy days mainly occurred in the intensive straw burning periods,

347 accounting for 76.4% of all rainy days in 2012. The frequent wet scavenging might have suppressed

348 the EC concentrations during the intensive straw burning periods, so that the annual EC level for

349 2012 was comparable to those recorded from 2011 onward.

350   Similar to OC and EC, the annual mean SO_2 and NO_2 concentrations also showed a decreasing

351 trend. As well-known, SO_2 originates from coal combustion and sulfur-containing oil (Seinfeld and

352 Pandis, 1998). With the replacement of coal for industrial facilities, residential heating and cooking

353 by clean energy (e.g., natural gases, electricity and lower sulfur content in oil), a clear decline in

354 annual SO_2 concentrations was observed in the Beijing area starting from 2002. As compared to

355 SO_2, the annual decreasing rate of NO_2 was relatively lower. Besides the power plants and other

356 boilers, traffic emissions are another major source of NO_2. The rapid increase of vehicle population

357 may partly offset the great effort in reducing coal consumption to lower the NO_2 level despite the

358 transition to more stringent traffic emission standards.

359 **3.3 Monthly and seasonal variations**

360   Fig. S1 shows the monthly mean OC and EC concentrations at our study site for the whole 5-

361 year period. Similar variations are observed with generally higher mean OC and EC levels in the

362 cold season (from November to February next year when the centralized urban residential heating

363 is provided) and lower ones in the warm season (from April to October). The highest average OC

364 and EC concentrations were 24.1 ± 18.7 μg/m^3 in December 2016 and 9.3 ± 8.5 μg/m^3 in December

365 2015, respectively. However, the lowest OC and EC levels were not observed in the warm months;

366 they were 5.0 ± 4.6 μg/m^3 in January, 2018 and 1.5 ± 1.7 μg/m^3 in December, 2017, respectively;

367 this was associated with both frequent occurrence of cold air mass and the implementation of a

368 winter radical pollution control action plan (Chen and Chen, 2019) in Beijing from November, 2017.

369 Overall, the increased fuel consumption for domestic heating in addition to unfavorable

370 meteorological conditions (lower mixing layer height, temperature inversion and calm wind) in the

371 colder months is considered to lead to higher OC and EC levels (Ji et al., 2014). In addition, the

372 lower air temperature in the cold months led to shifting the gas-particle equilibrium of semi-volatile

373 organic compounds (SVOCs) into the particle phase, leading to the higher OC levels. In the cold

374 months, the cold start of vehicles (5.64 million vehicles in Beijing at the end of 2017) also increased

375 the emission of OC. In the warm season, lower OC and EC levels were observed, which could be

376   attributed to the following factors: no extra energy consumed for domestic heating, strong wet

377   scavenging by frequent precipitation occurring in these months, and more unstable atmospheric

378   conditions favorable for pollutant dispersion; in addition, during this period, the monthly mean OC

379   and EC concentrations generally decreased from year to year. In contrast, for the cold season, the

380   monthly mean OC and EC concentrations did not show a clear decreasing trend from year to year.

381   In addition to the more intensive energy consumption in the cold season, the EC and OC levels

382   could also be enhanced strongly by regional transport and stagnant meteorology leading to ground

383   surface accumulation in the autumn and winter (Wang et al., 2019; Yi et al., 2019); this would have

384   counteracted the efficacy of the energy structure change in the Beijing-Tianjin-Hebei region in the

385   past few years. It is worth pointing out that, on a year to year basis, the monthly average OC and

386   EC concentrations in the cold seasons of 2017 and 2018 were generally lower than those in 2016,

387   demonstrating to some extent the effectiveness of the execution of the radical pollution control

388   measures for cities on the air pollution in the Beijing-Tianjin-Hebei region. The interquartile ranges

389   of OC and EC in the warm months were narrower than in the cold months, indicating that there was

390   more substantial variation in concentration in the latter months. The larger variation in the colder

391   months could be caused by the cyclic accumulation and scavenging processes. In this region, due to

392   these processes, the concentration of particulate matter increases rapidly when the air mass back

393   trajectories change from the northwest and north to the southwest and south over successive days in

394   Beijing; in contrast, the concentration of particulate matter declines sharply when a cold front causes

395   a shift of back trajectories from the southwest and south to the north and northwest (Ji et al., 2012).

396   The accumulation processes are closely associated with unfavorable meteorological conditions,

397   which give rise to higher OC and EC concentrations, while more scavenging of aerosols by cold

398   fronts leads to lower levels.

399   As to the seasonality in OC and EC, similar seasonal variations are observed in the various

400   years with generally higher mean concentrations in autumn and winter and lower levels in spring

401   and summer (Fig. 4). Remarkably, the OC and EC concentrations in the autumn and winter of 2017

402   were lower than those in the previous years. This was due to the combined effect of controlling

403   anthropogenic emissions strictly and favorable meteorological conditions. Since September 2017, a

404   series of the most stringent measures within the Action Plan on Prevention and Control of Air

405   Pollution was implemented to improve the air quality; these measures included restricting industrial

406   production by shutting down thousands of polluting plants, suspending the work of iron and steel

407   plants in 28 major cities and limiting the use of vehicles and reducing coal consumption as a heating

408   source in northern China. In addition, the air quality improvement in the autumn and winter of 2017

409   was closely tied to frequent cold fronts accompanied by strong winds, which was favorable for

410   dispersing the pollutants. The average OC and EC concentrations in the winter were 1.69 and 1.14,

411   2.17 and 1.93, 1.49 and 2.14, 2.41 and 2.29 and 0.80 and 0.88 times higher than those in the summer

412   for 2013, 2014, 2015, 2016 and 2017, respectively. The difference in the ratios for 2017 was due to

413   the series of the most stringent measures taking effect and favorable meteorology. The Beijing

414   municipal government in particular has made great efforts to replace coal by natural gases and

415   electricity-powered facilities. Besides, new energy vehicles are increasingly used to replace the

416   gasoline vehicles.

417   **3.4 Diurnal variation and weekly pattern for OC and EC**

418   As can be seen in Figs. S2 and S3, a clear diurnal variation is observed for both OC and EC in

419   each year. This variation is closely tied to the combined effect of diurnal variation in emission

420   strength and evolution of the PBL. The pattern for EC with higher concentrations in the nighttime

421   (from 20:00 to 4:00) and lower levels in the daytime (from 9:00 to 16:00) is largely linked to the

422   vehicular emissions. The EC concentrations increased starting from 17:00, corresponding with the

423   evening rush hours, emission from nighttime heavy-duty diesel trucks (HDDT) and heavy-duty

424   vehicles (HDV) and the formation of a nocturnal stable PBL. As regulated by the Beijing Traffic

425   management Bureau (http://www.bjjtgl.gov.cn/zhuanti/10weihao/), HDV and HDDT are allowed to

426   enter the urban area inside the 5th Ring Road from 0:00 to 06:00 (local Time). At other times, both

427   the higher PBL height and lower traffic intensity resulted in lower EC concentrations. The amplitude

428   of the diurnal variation in the EC concentrations was smaller in the last three years. The maximum

429   peak concentration (22:00-7:00) was 1.68, 1.62, 1.43, 1.40 and 1.40 times higher than that observed

430   in the valley period (13:00-15:00) for 2013, 2014, 2015, 2016 and 2017, respectively. Similar to EC,

431   the diurnal pattern for OC was also characterized by higher concentrations in the nighttime (from

432   20:00 to 4:00) and lower levels in the daytime (from 14:00 to 16:00). However, the formation of

433   secondary organic carbon from gas-phase oxidation of VOCs with increased solar radiation during

434   midday gave rise to a small additional peak of OC. Like for EC, the amplitude of the diurnal

435   variation in the OC concentrations was smaller in the last three years. The maximum peak

436   concentration (19:00-3:00) was 1.47, 1.47, 1.30, 1.34 and 1.26 times higher than that observed in

437   the valley period (14:00-16:00) for 2013, 2014, 2015, 2016 and 2017, respectively. It was pity that

438   no diurnal variation in traffic counts can be available but the hourly average traffic counts in 2015,

439   2016 and 2017 could be found in (Beijing Transportation Annual Report,

440   http://www.bjtrc.org.cn/JGJS.aspx?id=5.2&Menu=GZCG). Considering that the hourly average

441   traffic counts varied little in urban Beijing and they were 5969/hr, 5934/hr and 6049/hr in 2015,

442   2016 and 2017, respectively, the small amplitude of the diurnal variation in the last three years might

443   be related to local emission intensities; these might have been significantly affected by the

444   enforcement of a series of traffic emission control measures since 2015, including more strict

445   restriction of emission from heavy-duty diesel vehicle public buses, wider usage of electric public

446   buses, and scrappage of all the high-emitting (yellow-labelled) vehicles, etc. (Tab. S2). All these

447   actions led to a decline in emissions of OC and EC and narrowed the amplitude of the diurnal

448   variation in the EC concentration.

449   Separate diurnal variations of OC and EC for each season in each year are shown in Figs S4

450   and S5. Similar patterns are observed in in the four seasons but the difference between peak and

451   valley levels is larger in the winter than in the other three seasons. The larger variation in the winter

452   is due to the additional emission from residential heating and more unfavorable meteorological

453   conditions (Ji et al., 2016).

454   The difference in diurnal pattern between weekdays and weekends was also examined, see Figs.

455   S6 and S7. Similar diurnal variations are found on weekdays and weekend days. The maximum

456   peak concentration for EC (22:00-7:00) was 1.55, 1.43, 1.55, 1.51, 1.51, 1.46 and 1.59 times higher

457   than the valley concentration (13:00-15:00) for Monday, Tuesday, Wednesday, Thursday, Friday,

458   Saturday and Sunday, respectively, while the maximum peak concentration for OC (19:00-3:00)

459   was 1.41, 1.32, 1.38, 1.43, 1.37, 1.31 and 1.43 times higher than the valley concentration (14:00-

460   16:00) for Monday, Tuesday, Wednesday, Thursday, Friday, Saturday and Sunday, respectively. In

461   contrast to previous studies (Grivas et al., 2012; Jeong et al., 2017; Chang et al., 2017), OC and EC

462   exhibited statistically significant higher concentrations on weekends than on weekdays in this study

463   (statistically significant based on the analysis of the weekly data using *t*-test statistics, $p<0.05$). The

464   average OC and EC concentrations on Saturday and Sunday were 13.2 ± 11.8 μg/m^3 and 3.9 ± 2.7

465   μg/m^3 and 12.0 ± 10.4 μg/m^3 and 3.7 ± 3.6 μg/m^3, respectively, whereas the average OC and EC

466   levels during the weekdays were 11.8 ± 10.8 μg/m^3 and 3.6 ± 3.5 μg/m^3, respectively. This indicates

467   that there is no significant decline in anthropogenic activity in the weekends compared to weekdays.

468   In fact, enhanced anthropogenic emissions could be caused by no limit on driving vehicles based

469   on license plate on weekends. The larger OC and EC concentrations in the weekend are thus mainly

470   attributed to enhanced traffic emissions, which is consistent with higher NO_2 and CO concentrations

471   in the weekend (on average 56.6 ± 35.9 μg/m^3 for NO_2 and 1.16 ± 1.18 mg/m^3 for CO on weekdays

472   (number of samples = 29492); 57.8 ± 37.0 μg/m^3 for NO_2 and 1.25 ± 1.18 mg/m^3 for CO on

473   weekends (number of samples = 11881)).

474   **3.5 Relationship between OC and EC and with gaseous pollutants**

475   The relationship between particulate OC and EC is an important indicator that can give

476   information on the origin and chemical transformation of carbonaceous aerosols (Chow et al., 1996).

477   Primary OC and EC are mainly derived from vehicular emissions, coal combustion, biomass

478   burning, etc. in urban areas (Bond, et al., 2013). Primary OC and EC could correlate well with each

479   other under the same meteorology. However, the correlation would become gradually less

480   significant with the enhancement of secondary OC formation via complex chemical conversion of

481   VOCs (gas-to-particle or heterogeneous conversion). In addition, it should be noted that EC is more

482   stable than OC (Bond, et al., 2013). Hence, the relationship between OC and EC can to some extent

483   be used as a parameter reflecting the source types and contributions (Blando and Turpin, 2000). Fig.

484   5 presents the regression between the OC and EC concentrations for the PM$_{2.5}$ samples of the

485   separate years 2013 to 2017. Significant correlations (R^2 ranging from 0.87 to 0.66) were observed

486   with the slopes declining from 3.6 to 2.9 throughout the study period. The significant correlations

487   suggest that in most cases OC and EC originated from similar primary sources. The slopes are

488   consistent with the OC/EC ratios ranging from 2.0 to 4.0 for urban Beijing in previous studies (He

489   et al., 2001; Dan et al., 2004; Zhao et al., 2013; Ji et al., 2016). In addition, the average OC/EC

490   ratios observed in this study are comparable to those observed at other urban sites with vehicular

491   emission as a dominant source in China and foreign countries, but lower than those in cities where

492   coal is an important source of the energy needed (Table 3). The decline in the OC/EC ratio may be

493   caused by decline in coal consumption and restriction in biomass burning. Coal combustion,

494   biomass burning and secondary formation give rise to higher OC/EC ratios while vehicular emission

495   result in lower ones (Cao et al., 2005).

496   EC and part of the OC originate from primary anthropogenic emissions, including fossil fuel

497   combustion and biomass burning (Bond et al., 2013), and secondary OC is formed along with ozone

498   formation. Hence, long-term and concurrent measurement of OC, EC, SO_2, NO_x, CO and O_3 is

499   helpful for understanding the emission features or formation processes and for providing tests to

500   current emission inventories. The variation in the OC and EC as a function of the SO_2, NO_x, CO

501   and O_3 concentration is shown in Fig. 6. There is a clear increase in OC and EC with increasing

502   SO_2, NO_x and CO, suggesting that the latter played a role in the enhancement of the former and that

503   these various species shared common sources although they have a different lifetime. OC and EC

504   increased, on average, by approximately 8.9 $\mu g/m^3$ and 5.7 $\mu g/m^3$, respectively, with an increase of

505   2 mg/m^3 in CO. Considering that CO has a long lifetime (Liang et al., 2004) and that its increase

506   depends on source strength and meteorology, high CO concentrations usually occur in the heating

507   season when unfavorable meteorological conditions prevail. At very high CO concentrations, the

508   increase in OC becomes slower than that in EC. This can be explained by that local emissions

509   became dominant because the unfavorable meteorological conditions corresponding with the high

510   CO concentrations resulted in a weak exchange of air on the regional scale. The OC/EC ratio

511   declined at very high CO concentrations. This could be because vehicular emissions played an

512   important role in the OC and EC loadings (Ji et al., 2019). As documented by previous studies

513   (Schauer et al., 2002, Na et al., 2004), emission of gasoline vehicles results in an OC/EC ratio

514   varying from 3 to 5 while that of diesel vehicles is below 1. The above results are consistent with

515   previous studies which showed that gasoline and diesel vehicles give rise to higher CO emissions

516   (Wu et al., 2016).

517   Given that NO_x and CO have some common emission sources (Hassler et al., 2016), the OC

518   and EC levels were also analyzed in different intervals of NO_x concentrations. Both OC and EC are

519   enhanced with increasing NO_x concentrations. Their enhancements were 5.0 $\mu g/m^3$ and 2.1 $\mu g/m^3$,

520   respectively, for an increase in NO_x concentration of 40 $\mu g/m^3$. Although NO_x are highly reactive

521 and have a short lifetime (Seinfeld and Pandis, 1998) in contrast to CO, the OC/EC ratio also

522 declined at very high NO_x concentrations, be it to a lesser extent than was the case at very high CO

523 concentrations. As was the case for high CO concentrations, more stable meteorological conditions

524 and local emissions became prevailed when higher concentrations of NO_x were observed. In fact,

525 63.5 % of all NO_x emissions come from vehicular emissions based on the statistical data of air

526 pollutant emissions in Beijing

527 (http://www.bjepb.gov.cn/bjhrb/xxgk/ywdt/zlkz/hjtj37/827051/index.html).

528   Examining the variation of OC and EC for different intervals of SO_2 concentrations allows us

529 to further study the impacts of industrial production or coal combustion on the OC and EC levels.

530 Similar to the relationship between CO and the carbonaceous species, the OC and EC concentrations

531 enhanced with increasing SO_2 concentrations. Their enhancements were 2.8 μg/m^3 and 0.7 μg/m^3,

532 respectively, for an increase in SO_2 concentration of 10 μg/m^3. An increase in the OC/EC ratio

533 occurred at large SO_2 concentrations, suggesting that coal consumption provided a substantial

534 contribution to the OC and EC levels in Beijing. Because oil with a low sulfur content has been

535 widely used in Beijing since 2008 and little coal was used in the urban areas of Beijing, the SO_2

536 mostly originated from industrial production in the surrounding areas of Beijing and from coal

537 combustion for residential heating in the suburban and rural areas of Beijing. Previous studies also

538 showed that a higher OC/EC ratio is due to coal consumption and not from vehicular emissions

539 (Cao et al., 2005). Hence, coal combustion (for industrial production) on the regional scale led to

540 the enhancement of both the OC/EC ratio and SO_2 concentrations in Beijing via long-range transport.

541   Emissions of primary air pollutants lead through multiple pathways to the formation of ozone

542 and secondary organic carbon (SOC) (Seinfeld and Pandis, 1998), both of which are the principal

543 components of photochemical smog. The relationship between OC and O_3 is of use for

544 understanding their variation and formation. The OC concentrations were highest for an O_3

545 concentration of 50 μg/m^3, which is approximately the average O_3 concentration in Beijing in winter

546 (Cheng et al., 2018). During the period of an O_3 concentration of 50 μg/m^3, low atmospheric

547 temperature (9.4±9.9 ºC), relatively high RH (59.2±23.7 %), lower WS (1.1±0.8 m/s) and higher

548 NO_x concentrations (72.7±57.5 ppb) were observed and a lower mixed layer height was recorded in

549 winter (Tang et al., 2016), which were favorable for accumulation and formation of OC. A relatively

lower temperature is beneficial for condensation/absorption of SVOCs into existing particles (Ji et al., 2019), which would then experience further chemical reactions to generate secondary organic aerosol (SOA). Note that a low temperature does not significantly reduce SOA formation rates (Huang et al., 2014) in the winter. In addition, processes including aqueous-phase oxidation and NO_3-radical-initiated nocturnal chemistry may contribute to or even dominate SOA formation during winter (Hallquist et al., 2009; Rollins et al., 2012; Huang et al., 2014). Hence, the above factors gave rise to the higher OC concentration at an O_3 concentration of 50 μg/m^3 particularly in winter. In addition, scattering and absorbing effects of aerosols that were trapped in the lower mixed layer height led to less solar radiation reaching the ground and further restrained the O_3 formation in the cold season (Xing et al., 2017; Wang et al., 2016b). OC declined when O_3 concentrations increased from 50 to 100 μg/m^3. Usually moderate O_3 concentrations accompanying lower OC concentrations are caused by increasing T (19.5±8.3 ºC), increasing WS (2.0±1.3 m/s) and less titration of relatively lower observed NO concentrations (6.4±14.6 ppb). It can also be seen that there was a concurrent increasing trend of OC and ozone when the O_3 concentration was above 100 μg/m^3, which generally occurred in the warmer season. Besides the impact of meteorological conditions, such a trend might not be dominated by gas-to-particle partitioning of low-volatility organic compounds but by the oxidation of VOCs driven by hydroxyl radicals to generate both SOC and O_3 with relatively long lifetimes (>12 h; Wood et al., 2010).

3.6 Impact of atmospheric transport on the OC and EC concentrations

Figs. 7 and 8 show the results of the NWR analysis applied to 1-h PM$_{2.5}$-associated OC and EC concentrations measured from 2013 and 2017 in Beijing. Fig. S8 presents the gridded emissions of OC and BC for the Beijing-Tianjin-Hebei (BTH) region and China, based on emission inventory (Zheng et al., 2018). The NWR results exhibit distinct hot spots (higher concentrations) in the northeast wind sector at wind speeds of approximately 0-6 km/h, which were closely associated with local emissions under stagnant meteorological conditions (low wind speed), as well as diffuse signals in the southwestern wind sector. The joint probability data in Figs. 7 and 8 show prevailing winds were from N to E and from S to W with wind speeds of approximately 1-6 km/h and of approximately 4-9 km/h, respectively. Note further that the hot spots of OC are broader than those of EC in the graphs of estimated concentrations; this might be due to the fact that the VOCs (the

579 precursors of SOC) emitted from upwind areas at the relatively higher WS in contrast to EC,

580 including the SW wind sector, led to an increase in OC concentrations at the receptor site while the

581 EC concentrations slowly declined due to dilution and deposition.

582 Considering that the NWR analysis can only provide an allocation of local sources, the PSCF

583 analysis is a helpful complement to investigate potential advection of pollution over larger

584 geographical scales (Petit et al., 2017). Fig. 9 presents the PSCF results for OC and EC for the years

585 2013 to 2017. Similar to the NWR analysis, the PSCF results indicated that local emissions and

586 regional transport from southerly areas were important contributors to the OC and EC loadings

587 during the whole study period. Only slight differences in the potential source regions are observed

588 between the different years. In 2013, a clear high potential source area was recorded for both OC

589 and EC; it was located in the southern plain areas of Beijing, particularly in the adjacent areas of

590 the Hebei, Henan, Shandong, Anhui and Jiangsu provinces. This was because there were intensified

591 anthropogenic emissions from those in 2013. The high pollutant emissions were caused by rapid

592 economic growth, urbanization and increase in vehicle population, energy consumption and

593 industrial activity in the southern plain areas of Beijing (Zhu et al., 2018), which resulted in a high

594 aerosol loading in the downwind areas. This result is consistent with previous studies (Ren et al.,

595 2004; Wu et al., 2014; Ji et al., 2018). In contrast to 2013, in the years 2014 to 2017 the high potential

596 source regions for OC and EC stretched to the juncture of Inner Mongolia and the Shaanxi and

597 Shanxi provinces, and even to the juncture of Inner Mongolia and the Ningxia Hui Autonomous

598 Region and of Inner Mongolia and the Gansu province. This is consistent with coal power plants

599 being abundant in the above areas (Liu F. et al., 2015). As well known, coal power plants are also

600 important emitters of SO_2, and those emissions were seen in satellite images (Li et al., 2017; Zhang

601 et al., 2017), thus proving evidence for those sources. The potential source areas for OC and EC

602 were similar in 2013 and 2014. Overall, the potential source areas were more intense for OC than

603 for EC. The emission of OC precursors (i.e., volatile organic compounds) from the Hebei, Henan,

604 Shandong, Anhui, Jiangsu, Shanxi and Shaanxi provinces led to OC concentrations downwind via

605 chemical conversion during the atmospheric transport. The widest potential source areas for OC and

606 EC were recorded in 2016 and they expanded into the eastern areas of Xinjiang Uyghur Autonomous

607 Region. They are probably associated with the economic boom in the western areas of China. In

2015, the potential source areas were like in 2013 and 2014 also more intense for OC than for EC. Although the winter action plan was enforced in Beijing, Tianjin and 26 surrounding cities (the so-called "2+26 cities"), whereby the industrial output was curtailed, inspections of polluting factories were ramped up and small-scale coal burning was banned at the end of 2017, there was still a clear spatial difference in emission of air pollutants, with relatively higher $PM_{2.5}$ concentrations in the southern areas of Beijing. Hence, these areas still contributed substantially to OC and EC loading in Beijing.

As found in earlier studies (Ji et al., 2018; Zhu et al., 2018), the southern areas of Beijing were main source areas. Despite the ever-stringent air pollution control measures, which are enforced in key areas of China, the economic booming in the western areas of China gave rise to substantial air pollution in the adjacent areas of several provinces and the northwestern areas of China. To further improve the air quality in Beijing, strict emission restrictions should be launched in the above areas and joint control and prevention of air pollution should be enforced on the regional scale. It should be avoided that polluted enterprises, which are closed in key regions, are moved to the western areas of China or to areas where there is no supervision and control of the emission of air pollutants.

4 Conclusions

In this study, hourly mass concentrations of OC and EC in $PM_{2.5}$ were semi-continuously measured from March 1, 2013 to February 28, 2018 at a study site in Beijing. The inter-annual, monthly, seasonal and diurnal variations in OC and EC are presented, the relationship between the carbonaceous species and other pollutants was examined and the source regions were assessed using both NWR and PSCF analysis. The impact of the air pollution control measures and of the regional transport on carbonaceous species in the fine particulate matter was investigated. The following main conclusions can be drawn:

(1) OC and EC occupied a high fraction of the observed $PM_{2.5}$ concentrations, making it a dominant contributor of $PM_{2.5}$. Their concentrations increased with the degrading air quality whereas their percentage in $PM_{2.5}$ declined, which was consistent with previous studies showing that secondary inorganic ions played a relatively more important role in increasing $PM_{2.5}$ concentrations.

(2) A clear decline in OC and EC levels was observed after a series of energy policies for air pollution abatement and control had been implemented. To further improve air quality, more

synergistic air pollution abatement measures of carbonaceous aerosols and VOCs emissions are needed.

(3) OC and EC showed marked seasonal, monthly, weekly and diurnal variations. The seasonal patterns were characterized by higher concentrations in the colder months (from November to February) and lower ones in the warm months (from May to October) of the various years. Because of stringent measures for air pollution abatement, the difference between the winter and summer levels decreased. The EC diurnal pattern was characterized by higher concentrations in the nighttime (from 20:00 to 4:00) and lower ones in the daytime (from 9:00 to 16:00). The higher OC and EC levels during the weekend can be attributed to the traffic regulation in Beijing. The diurnal fluctuation in OC and EC was closely tied to a combined effect of change in emission sources and evolution of the PBL.

(4) Significant correlations between OC and EC were observed throughout the study period, suggesting that OC and EC originated from common sources, such as vehicle exhaust, coal combustion, etc. The contribution of coal combustion and biomass burning decreased and this resulted in lower OC/EC ratios. The OC and EC concentrations increased with higher SO_2, CO and NO_x levels, while the O_3 and OC concentrations increased simultaneously for O_3 levels above 50 $\mu g/m^3$.

(5) Local emissions and regional transport played an important role in the OC and EC concentrations. Higher concentrations were observed for winds from the northeast sector at wind speeds of approximately 5 km/h, but there were also diffuse signals in the southwestern wind sectors. The potential source regions of OC and EC stretched to the broader areas in northwestern and western regions where coal and coal power plants are abundant. Some slight differences in the potential source regions were observed from 2013 to 2017, which was closely associated with the economic boom in the western areas of China. In addition, the southern areas of Beijing still contributed a lot to OC and EC loading in Beijing.

In summary, this study will be helpful for improving the understanding the sources of OC and EC associated with $PM_{2.5}$ and for assessing the effectiveness of local and national PM control measures. In addition, it provides valuable datasets for modelling studies and for assessing the health risk.

24

Author contributions

D.S., W.M. and Y.S. designed the research. D.S., W.M., J.H., Z.W., W. K., W.P., Y.S., J.Y., B.H. and Y.S. performed the research. D.S., Z.W., and W.M. analyzed the data. D.S., J.H., and W.M. wrote and edited the manuscript. All other authors commented on the manuscript.

References

Ashbaugh, L. L., Malm, W. C., and Sadeh, W. Z.: A residence time probability analysis of sulfur concentrations at Grand Canyon National Park, Atmos. Environ., 19, 1263-1270, 1985.

Bisht, D. S., Srivastava, A. K., Pipal, A. S., Srivastava, M. K., Pandey, A. K., Tiwari, S., and Pandithurai, G.: Aerosol characteristics at a rural station in southern peninsular India during CAIPEEX-IGOC: physical and chemical properties, Environ. Sci. Pollut. Res., 22, 5293-5304, 10.1007/s11356-014-3836-1, 2015.

Blando, J. and Turpin, B.: Secondary organic aerosol formation in cloud and fog droplets: a literature evaluation of plausibility, Atmos. Environ., 34 (10), 1623–1632, 2000.

Bond, T. C., Doherty, S. J. Fahey, D. W., Forster, P. M., Berntsen, T., DeAngelo, B. J., Flanner, M. G., Ghan, S., Kärcher, B., Koch, D., Kinne, S., Kondo, Y., Quinn, P. K., Sarofim, M. C., Schultz, M. G., Schulz, M., Venkataraman, C., Zhang, H., Zhang, S., Bellouin, N., Guttikunda, S. K., Hopke, P. K., Jacobson, M. Z., Kaiser, J. W., Klimont, Z., Lohmann, U., Schwarz, J. P., Shindell, D., Storelvmo, T., Warren, S. G., and Zender, C. S.: Bounding the role of black carbon in the climate system: A scientific assessment, J. Geophys. Res-Atmos., 118(11), 5380–5552, 2013.

Boström, C. E., Gerde, P., Hanberg, A., Jernström, B., Johansson, C., Kyrklund, T., Rannug, A.,

Torngvist, M., Victorin, K., and Westerholm, R.: Cancer risk assessment, indicators, and guidelines for polycyclic aromatic hydrocarbons in the ambient air, Environ. Health Perspect., 110, 451-488, 2002.

Boucher, O., Randall, D., Artaxo, P., Bretherton, C., Feingold, G., Forster, P., Kerminen, V. M., Kondo, Y., Liao, H., Lohmann, U., Rasch, P., Satheesh, S. K., Sherwood, S., Stevens, B., Zhang, X. Y.: Contribution of working group | to the fifth assessment report of the Intergovernmental Panel on Climate Change. Clouds and aerosols. In: Stocker, T. F., Qin, D., Plattner, G. K., Tignor, M., Allen, S. K., Doschung, J., Nauels, A., Xia, Y., Bex, V., Midgley, P. M., Eds. Climate change 2013: the physical science basis. Cambridge University Press, Cambridge, United Kingdom and New York, 616–617, 2013.

Bressi, M., Sciare, J., Ghersi, V., Bonnaire, N., Nicolas, J. B., Petit, J. E., Moukhtar, S., Rosso, A., and Féron, A.: A one-year comprehensive chemical characterisation of fine aerosol ($PM_{2.5}$) at urban, suburban and rural background sites in the region of Paris (France), Atmos. Chem. Phys., 13(15), 7825-7844, 2013.

Cao, J. J., Lee, S. C., Zhang, X. Y., Chow, J. C., An, Z. S., Ho, K. F., Watson, J. G., Fung, K., Wang, Y. Q., and Shen, Z. X.: Characterization of airborne carbonate over a site near Asian dust source regions during spring 2002 and its climatic and environmental significance, J. Geophys. Res.: Atmos., 110, doi:10.1029/2004JD005244, 2005.

Chang, Y., Deng, C., Cao, F., Cao, C., Zou, Z., Liu, S., Lee, X., Li, J., Zhang, G., and Zhang, Y.: Assessment of carbonaceous aerosols in Shanghai, China – Part 1: long-term evolution, seasonal variations, and meteorological effects, Atmos. Chem. Phys., 17, 9945-9964, https://doi.org/10.5194/acp-17-9945-2017, 2017.

Chen, D., Cui, H., Zhao, Y., Yin, L., Lu, Y., and Wang, Q.: A two-year study of carbonaceous aerosols in ambient $PM_{2.5}$ at a regional background site for western Yangtze River Delta, China, Atmos. Res., 183, 351-361, 2017.

Chen, H. and Chen, W.: Potential impact of shifting coal to gas and electricity for building sectors in 28 major northern cities of China. Appl. Energ., 236, 1049-1061, 2019.

Chen, X. C., Ward, T. J., Cao, J. J., Lee, S. C., Chow, J. C., Lau, G. N. C., Yim, S. H. L., and Ho, K. F.: Determinants of personal exposure to fine particulate matter ($PM_{2.5}$) in adult subjects in Hong

Kong, Sci. Total Environ., 628-629, 1165-1177, https://doi.org/10.1016/j.scitotenv.2018.02.049, 2018.

Chen, Y., Xie, S., Luo, B., and Zhai, C.: Characteristics and origins of carbonaceous aerosol in the Sichuan Basin, China, Atmos. Environ., 94, 215-223, 2014.

Chen, Y., Xie, S. D., Luo, B., and Zhai, C. Z.: Particulate pollution in urban Chongqing of southwest China: Historical trends of variation, chemical characteristics and source apportionment, Sci. Total Environ., 584, 523-534, 2017

Cheng, N., Chen, Z., Sun, F., Sun, R., Dong, X., Xie, X., and Xu, C.: Ground ozone concentrations over Beijing from 2004 to 2015: Variation patterns, indicative precursors and effects of emission reduction, Environ. Pollut., 237, 262-274, https://doi.org/10.1016/j.envpol.2018.02.051, 2018.

Chow, J. C., Watson, J. G., Lu, Z., Lowenthal, D. H., Frazier, C. A., Solomon, P. A., Thuillier, R. H., and Magliano, K.: Descriptive analysis of $PM_{2.5}$ and PM_{10} at regionally representative locations during SJVAQS/AUSPEX, Atmos. Environ., 30, 2079-2112, https://doi.org/10.1016/1352-2310(95)00402-5, 1996.

Dai, Q. L., Bi, X. H., Liu, B. S., Li, L. W., Ding, J., Song, W. B., Bi, S. Y., Schulze, B. C., Song, C. B., Wu, J. H., Zhang, Y. F., Feng, Y. C., and Hopke, P. K.: Chemical nature of $PM_{2.5}$ and PM_{10} in Xi'an, China: Insights into primary emissions and secondary particle formation, Environ. Pollut. 240, 155-166, 2018.

Dan, M., Zhuang, G., Li, X., Tao, H., and Zhuang, Y.: The characteristics of carbonaceous species and their sources in $PM_{2.5}$ in Beijing, Atmos. Environ., 38, 3443-3452, https://doi.org/10.1016/j.atmosenv.2004.02.052, 2004.

Ding, A. J., Huang, X., Nie, W., Sun, J. N., Kerminen, V. M., Petäjä, T., Su, H., Cheng, Y. F., Yang, X. Q., Wang, M. H., Chi, X. G., Wang, J. P., Virkkula, A., Guo, W. D., Yuan, J., Wang, S. Y., Zhang, R. J., Wu, Y. F., Song, Y., Zhu, T., Zilitinkevich, S., Kulmala, M., and Fu, C. B.: Enhanced haze pollution by black carbon in megacities in China, Geophys. Res. Lett., 43, 2873–2879, 2016.

Duan, F., He, K., Ma, Y., Yang, F., Yu, X., Cadle, S., Chan, T., and Mulawa, P.: Concentration and chemical characteristics of $PM_{2.5}$ in Beijing, China: 2001–2002, Sci. Total Environ., 355, 264-275, 2006.

Gao, J., Woodward, A., Vardoulakis, S., Kovats, S., Wilkinson, P., Li, L., Xu, L., Li, J., Yang, J., Li,

752   J., Cao, L., Liu, X., Wu, H., and Liu, Q.: Haze, public health and mitigation measures in China: A

753   review of the current evidence for further policy response, Sci. Total Environ., 578, 148-157,

754   https://doi.org/10.1016/j.scitotenv.2016.10.231, 2017.

755   Giglio, L.: MODIS Collection 5 Active Fire Product User's Guide Version 2.5

756   http://earthdata.nasa.gov/files/MODIS_Fire_Users_Guide_2.5.pdf, 2013.

757   Grivas, G., Cheristanidis, S., and Chaloulakou, A.: Elemental and organic carbon in the urban

758   environment of Athens. Seasonal and diurnal variations and estimates of secondary organic carbon,

759   Sci. Total Environ., 414, 535-545, 2012.

760   Hallquist, M., Wenger, J., Baltensperger, U., Rudich, Y., Simpson, D., Claeys, M., Dommen, J.,

761   Donahue, N. M., George, C., Goldstein, A. H., Hamilton, J. F., Herrmann, H., Hoffmann, T., Iinuma,

762   Y., Jang, M., Jenkin, M. E., Jimenez, J. L., Kiendler-Scharr, A., Maenhaut, W., McFiggans, G.,

763   Mentel, Th. F., Monod, A., Prevot, A. S. H., Seinfeld, J. H., Surratt, J. D., Szmigielski, R., and Wildt,

764   J.: The formation, properties and impact of secondary organic aerosol: current and emerging issues,

765   Atmospheric Chemistry and Physics 9(14), 5155-5236, 2009.

766   Hassler, B., McDonald, B. C., Frost, G. J., Borbon, A., Carslaw, D. C., Civerolo, K., Granier, C.,

767   Monks, P. S., Monks, S., Parrish, D. D., Pollack, I. B., Rosenlof, K. H., Ryerson, T. B.,

768   Schneidemesser, E., and Trainer, M.: Analysis of long-term observations of NOx and CO in

769   megacities and application to constraining emissions inventories, Geophys. Res. Lett., 43, 9920-

770   9930, doi:10.1002/2016GL069894, 2016.

771   He, K., Yang, F., Ma, Y., Zhang, Q., Yao, X., Chan, C. K., Cadle, S., Chan, T., and Mulawa, P.: The

772   characteristics of $PM_{2.5}$ in Beijing, China, Atmos. Environ., 35, 4959-4970,

773   https://doi.org/10.1016/S1352-2310(01)00301-6, 2001.

774   He, K. B., Yang, F. M., Duan, F. K., Ma Y. L.: Atmospheric particulate matter and regional complex

775   pollution, Science Press, Beijing, China. 310-327, 2011.

776   Henry, R., Norris, G. A., Vedantham, R., and Turner, J. R.: Source region identification using

777   Kernel smoothing, Environ. Sci. Technol., 43 (11), 4090-4097, http://dx.doi.org/10.1021/

778   es8011723, 2009.

779   Hu, G., Sun, J., Zhang, Y., Shen, X., and Yang, Y.: Chemical composition of $PM_{2.5}$ based on two-

780   year measurements at an urban site in Beijing. Aerosol Air Qual. Res, 15, 1748-1759, 2015.

781 Huang, R. J., Zhang, Y. L., Bozzetti, C., Ho, K. F., Cao, J. J., Han, Y. M., Dällenbach, K. R., Slowik,
782 J. G., Platt, S. M., Canonaco, F., Zotter, P., Wolf, R., Pieber, S. M., Bruns, E. A., Crippa, M., Ciarelli,
783 G., Piazzalunga, A., Schwikowski, M., Abbaszade, G., Schnelle-Kreis, J., Zimmermann, R., An, Z.
784 S., Szidat, S., Baltensperger, U., EI Haddad, I., and Prévôt, A. S. H.: High secondary aerosol
785 contribution to particulate pollution during haze events in China, Nature, 514, 218-222, 2014.
786 Jeong, B., Bae, M. S., Ahn, J., and Lee, J.: A study of carbonaceous aerosols measurement in
787 metropolitan area performed during Korus-AQ 2016 campaign, J. Kor. Soc. Atmos. Environ., 33,
788 2017.
789 Ji, D., Li, L., Wang, Y., Zhang, J., Cheng, M., Sun, Y., Liu, Z. R., Wang, L. L., Tang, G. Q., Hu, B.,
790 Chao, N., Wen, T. X., and Miao, H. Y.: The heaviest particulate air-pollution episodes occurred in
791 northern China in January, 2013: Insights gained from observation, Atmos. Environ., 92, 546-556,
792 2014.
793 Ji, D. S., Wang, Y. S., Wang, L. L., Chen, L. F., Hu, B., Tang, G. Q., Xin, J. Y., Song, T., Wen, T. X.,
794 Sun, Y., Pan, Y. P., and Liu, Z. R.: Analysis of heavy pollution episodes in selected cities of northern
795 China, Atmos. Environ., 50, 338-348, 2012.
796 Ji, D. S., Zhang, J. K., He, J., Wang, X. J., Pang, B., Liu, Z. R., Wang, L. L., and Wang, Y. S.:
797 Characteristics of atmospheric organic and elemental carbon aerosols in urban Beijing, China,
798 Atmos. Environ., 125, 293-306, 2016.
799 Ji, D. S., Yan, Y. C., Wang, Z. S., He, J., Liu, B., Sun, Y., Gao, M., Li, Y., Cao, W., Cui, Y., Hu, B.,
800 Xin, J. Y., Wang, L. L., Liu, Z. R., Tang, G. Q., and Wang, Y. S.: Two-year continuous measurements
801 of carbonaceous aerosols in urban Beijing, China: Temporal variations, characteristics and source
802 analyses, Chemosphere, 200, 191-200, 2018.
803 Ji, D. S., Gao, M., Maenhaut, W., He, J., Wu, C., Cheng, L. J., Gao, W. K., Sun, Y., Sun, J. R., Xin,
804 J. Y., Wang, L. L., and Wang, Y. S.: The carbonaceous aerosol levels still remain a challenge in the
805 Beijing-Tianjin-Hebei region of China: Insights from continuous high temporal resolution
806 measurements in multiple cities, Environ. Int., 126: 171-183, 2019.
807 Jin, Y., Andersson, H., and Zhang, S.: Air pollution control policies in China: a petrospective and
808 prospects, Int. J. Env. Res. Pub. He., 13(12), 1219, 2016.
809 Lang, J., Zhang, Y., Zhou, Y., Cheng, S., Chen, D., Guo, X., Chen, S., Li, X. X., Xing, X. F., and

810   Wang, H. Y.: Trends of $PM_{2.5}$ and chemical composition in Beijing, 2000-2015, Aerosol Air Qual.

811   Res., 17, 412-425, 2017.

812   Li, B., Zhang, J., Zhao, Y., Yuan, S., Zhao, Q., Shen, G., and Wu, H.: Seasonal variation of urban

813   carbonaceous aerosols in a typical city Nanjing in Yangtze River Delta, China, Atmos. Environ.,

814   106, 223-231, 2015.

815   Li, C., Chen, P., Kang, S., Yan, F., Hu, Z., Qu, B., and Sillanpää, M.: Concentrations and light

816   absorption characteristics of carbonaceous aerosol in $PM_{2.5}$ and PM_{10} of Lhasa city, the Tibetan

817   Plateau, Atmos. Environ., 127, 340-346, https://doi.org/10.1016/j.atmosenv.2015.12.059, 2016.

818   Li, C., McLinden, C., Fioletov, V., Krotkov, N., Carn, S., Joiner, J., Streets, D., He, H., Ren, X., Li,

819   Z., and Dickerson, R.: India is overtaking China as the world's largest emitter of anthropogenic

820   sulfur dioxide, Scientific Reports, DOI:10.1038/s41598-017-14639-8, 2017.

821   Li, Y. C., Shu, M., Ho, S. S. H., Yu, J. Z., Yuan, Z. B., Liu, Z. F., Wang, X. X., and Zhao, X, Q.:

822   Effects of chemical composition of $PM_{2.5}$ on visibility in a semi-rural city of Sichuan Basin, Aerosol

823   and Air Qual. Res., 18(4): 957-968, 2018.

824   Liang, Q., Jaeglé, L., Jaffe, D. A., Weiss-Penzias, P., Heckman, A., and Snow, J. A.: Long-range

825   transport of Asian pollution to the northeast Pacific: Seasonal variations and transport pathways of

826   carbon monoxide, J. Geophys. Res-Atmos., 109, doi:10.1029/2003JD004402, 2004.

827   Liu, D., Li, J., Zhang, Y., Xu, Y., Liu, X., Ding, P., Shen, C., Chen, Y., Tian, C., and Zhang, G.: The

828   use of levoglucosan and radiocarbon for source apportionment of $PM_{2.5}$ carbonaceous aerosols at a

829   background site in east China, Environ. Sci. Technol., 47, 10454, 2013.

830   Liu, F., Zhang, Q., Tong, D., Zheng, B., Li, M., Huo, H., and He, K. B.: High-resolution inventory

831   of technologies, activities, and emissions of coal-fired power plants in China from 1990 to 2010,

832   Atmos. Chem. Phys., 15, 13299-13317, https://doi.org/10.5194/acp-15-13299-2015, 2015.

833   Liu, G., Li, J., Wu, D., and Xu, H.: Chemical composition and source apportionment of the ambient

834    $PM_{2.5}$ in Hangzhou, China, Particuology, 18, 135-143, 2015.

835   Lupu A. and Maenhaut, W.: Application and comparison of two statistical trajectory techniques for

836   identification of source regions of atmospheric aerosol species, Atmos. Environ., 36, 5607-5618,

837   2002.

838   Lv, B., Zhang, B., and Bai, Y.: A systematic analysis of $PM_{2.5}$ in Beijing and its sources from 2000

839   to 2012. Atmos. Environ., 124, 98-108, 2016.

840   Malm, W. C., Sisler, J. F., Huffman, D., Eldred, R. A., and Cahill, T. A.: Spatial and seasonal trends

841   in particle concentration and optical extinction in the United States, J. Geophys. Res-Atmos., 99,

842   1347-1370, doi:10.1029/93JD02916, 1994.

843   Miyakawa, T., Kanaya, Y., Komazaki, Y., Miyoshi, T., Nara, H., Takami, A., Moteki, N., Koike, M.,

844   and Kondo, Y.: Emission regulations qltered the concentrations, origin, and formation of

845   carbonaceous aerosols in the Tokyo metropolitan area, Aerosol Air Qual. Res., 16, 1603-1614,

846   10.4209/aaqr.2015.11.0624, 2016.

847   Na, K., Sawant, A. A., Song, C., and Cocker, D. R.: Primary and secondary carbonaceous species

848   in the atmosphere of Western Riverside County, California, Atmos. Environ., 38, 1345-1355,

849   https://doi.org/10.1016/j.atmosenv.2003.11.023, 2004.

850   Niu, X. Y., Cao, J. J., Shen, Z. X., Ho, S. S. H., Tie, X. X., Zhao, S. Y., Xue, H. M., Zhang, T., and

851   Huang, R. J.: $PM_{2.5}$ from the Guanzhong Plain: Chemical composition and implications for emission

852   reductions, Atmos. Environ., 147, 458-469, 2016.

853   Paraskevopoulou, D., Liakakou, E., Gerasopoulos, E., Theodosi, C., and Mihalopoulos, N.: Long-

854   term characterization of organic and elemental carbon in the $PM_{2.5}$ fraction: the case of Athens,

855   Greece, Atmos. Chem. Phys., 14(23), 13313-13325, 2014.

856   Park, J. S., Song, I. H., Park, S. M., Shin, H., and Hong, Y.: The characteristics and seasonal

857   variations of OC and EC for $PM_{2.5}$ in Seoul metropolitan area in 2014, J. Environ. Impact Assess.,

858   24, 578-592, 2015.

859   Peltier, R. E., Weber, R. J., and Sullivan, A. P.: Investigating a liquid-based method for online

860   organic carbon detection in atmospheric particles, Aerosol Sci. Tech., 41, 1117-1127,

861   10.1080/02786820701777465, 2007.

862   Pereira, G. M., Teinilä, K., Custódio, D., Santos, A. G., Xian, H., Hillamo, R., Alves, C. A., Andrade,

863   J. B., Rocha, G. O., Kumar, P., Balasubramanian, R., Andrade M. F., and Vasconcellos, P. C.:

864   Airborne particles in the Brazilian city of São Paulo: One-year investigation for the chemical

865   composition and source apportionment, Atmos. Chem. Phys., 17, 11943-11969, 2017.

866   Petit, J. E., Favez, O., Albinet, A., and Canonaco, F.: A user-friendly tool for comprehensive

evaluation of the geographical origins of atmospheric pollution: Wind and trajectory analyses. Environ. Modell. Softw., 88, 183-187, 2017.

Poirot, R. L. and Wishinski, P. R.: Visibility, sulfate and air mass history associated with the summertime aerosol in northern Vermont, Atmos. Environ., 20, 1457-1469, 1986.

Polissar, A. V., Hopke, P. K., and Harris, J. M.: Source regions for atmospheric aerosol measured at Barrow, Alaska, Environ. Sci. Technol., 35, 4214-4226, 2001.

Ram, K. and Sarin, M. M.: Spatio-temporal variability in atmospheric abundances of EC, OC and WSOC over Northern India, J. Aerosol Sci., 41, 88-98, https://doi.org/10.1016/j.jaerosci.2009.11.004, 2010.

Ram, K. and Sarin, M.: Carbonaceous aerosols over Northern India: sources and spatio-temporal variability, Proc. Indian Natn. Sci. Acad., 78, 523-533, 2012.

Ren, Z. H., Wan, B. T., Yu, T., Su, F. Q., Zhang, Z. G., Gao, Yang, X. X., Hu, H. L., Wu, Y. H., Hu, F., and Hong, Z. X.: Influence of weather system of different scales on pollution boundary layer and the transport in horizontal current field, Res. Environ. Sci., 17(1), 7-13, 2004.

Rollins, A. W., Browne, E. C., Min, K. E., Pusede, S. E., Wooldridge, P. J., Gentner, D. R., Goldstein, A. H., Liu, S., Day, D. A., Russell, L. M., and Cohen, R. C.: Evidence for NOx control over nighttime SOA formation, Science 337(6099), 1210-1212, 2012.

Schauer, J. J., Kleeman, M. J., Cass, G. R., and Simoneit, B. R.: Measurement of emissions from air pollution sources. 5. C1-C32 organic compounds from gasoline-powered motor vehicles, Environ. Sci. Technol., 36, 1169–1180, 2002.

Seinfeld, J. H. and Pandis, S. N.: Atmospheric chemistry and physics: from air pollution to climate change, John Wiley & Sons, 1998.

Shah, J. J., Johnson, R. L., Heyerdahl, E. K., and Huntzicker, J. J.: Carbonaceous aerosol at urban and rural sites in the United States, J. Air Pollut. Control Assoc., 36, 254-257, 1986.

Sharma, S. K. and Mandal, T. K.: Chemical composition of fine mode particulate matter ($PM_{2.5}$) in an urban area of Delhi, India and its source apportionment, Urban Clim., 21, 106-122, https://doi.org/10.1016/j.uclim.2017.05.009, 2017.

Shi, G. L., Peng, X., Liu, J. Y., Tian, Y. Z., Song, D. L., Yu, H. F., Feng, Y. C., and Russell, A. G.: Quantification of long-term primary and secondary source contributions to carbonaceous aerosols,

896   Environ. Pollut. 219, 897-905, 2016.

897   Sofowote, U. M., Rastogi, A. K., Debosz, J., and Hopke, P. K.: Advanced receptor modeling of

898   near–real–time, ambient $PM_{2.5}$ and its associated components collected at an urban–industrial site

899   in Toronto, Ontario, Atmos. Pollut. Res., 5, 13-23, https://doi.org/10.5094/APR.2014.003, 2014.

900   Song, Y., Xie, S., Zhang, Y., Zeng, L., Salmon, L. G., and Zheng, M.: Source apportionment of

901    $PM_{2.5}$ in Beijing using principal component analysis/absolute principal component scores and

902   UNMIX, Sci. Total Environ., 372, 278-286, 2006.

903   Tang, G., Zhang, J., Zhu, X., Song, T., Münkel, C., Hu, B., Schäfer, K., Liu, Z., Zhang, J., Wang,

904   L., Xin, J., Suppan, P., and Wang, Y.: Mixing layer height and its implications for air pollution over

905   Beijing, China, Atmos. Chem. Phys., 16, 2459-2475, https://doi.org/10.5194/acp-16-2459-2016,

906   2016.

907   Tao, J., Cheng, T., Zhang, R., Cao, J., Zhu, L., Wang, Q., Luo, L., and Zhang, L.: Chemical

908   composition of $PM_{2.5}$ at an urban site of Chengdu in southwestern China, Adv. Atmos. Sci., 30,

909   1070-1084, 2013.

910   Tao, J., Gao, J., Zhang, L., Zhang, R., Che, H., Zhang, Z., Lin, Z., Jing, J., Cao, J., and Hsu, S. C.:

911    $PM_{2.5}$ pollution in a megacity of southwest China: source apportionment and implication, Atmos.

912   Chem. Phys., 14, 2014.

913   Tao, J., Zhang, L., Cao, J., and Zhang, R.: A review of current knowledge concerning $PM_{2.5}$

914   chemical composition, aerosol optical properties and their relationships across China, Atmos. Chem.

915   Phys., 17(15), 9485-9518, 2017.

916   Villalobos, A. M., Amonov, M. O., Shafer, M. M., Devi, J. J., Gupta, T., Tripathi, S. N., Rana, K. S.,

917   McKenzie, M., Bergin, M. H., and Schauer, J. J.: Source apportionment of carbonaceous fine

918   particulate matter ($PM_{2.5}$) in two contrasting cities across the Indo–Gangetic Plain, Atmos. Pollut.

919   Res., 6, 398-405, https://doi.org/10.5094/APR.2015.044, 2015.

920   Wang, C., An, X., Zhang, P., Sun, Z., Cui, M., and Ma, L.: Comparing the impact of strong and

921   weak East Asian winter monsoon on $PM_{2.5}$ concentration in Beijing, Atmos. Res., 215, 165-177,

922   2019.

923   Wang, J., Allen, D. J., Pickering, K. E., Li, Z., and He, H.: Impact of aerosol direct effect on East

924   Asian air quality during the EAST‑AIRE campaign, J. Geophys. Res-Atmos., 121(11), 6534-6554,

925   2016b.

926   Wang, L., Zhou, X., Ma, Y., Cao, Z., Wu, R., and Wang, W.: Carbonaceous aerosols over China-

927   review of observations, emissions, and climate forcing, Environ. Sci. Pollut. Res., 23(2), 1671-1680,

928   2016a.

929   Wang, P., Cao, J. J., Shen, Z. X., Han, Y. M., Lee, S. C., Huang, Y., Zhu, C. S., Wang, Q. Y., Xu, H.

930   M., and Huang, R. J.: Spatial and seasonal variations of $PM_{2.5}$ mass and species during 2010 in Xi'an,

931   China, Sci. Total Environ., 508, 477-487, https://doi.org/10.1016/j.scitotenv.2014.11.007, 2015.

932   Wang, Y., Khalizov, A., Levy, M., and Zhang, R. Y.: New Directions: light absorbing aerosols and

933   their atmospheric impacts, Atmos. Environ., 81, 713–715, 2013.

934   Wang, Y. Q., Zhang, X. Y., and Draxler, R. R.: TrajStat: GIS-based software that uses various

935   trajectory statistical analysis methods to identify potential sources from long-term air pollution

936   measurement data, Environ. Modell. Softw., 24(8), 938-939, 2009.

937   Wang, Z. S., Zhang, D. W., Liu, B. X., Li, Y. T., Chen, T., Sun, F., Yang, D. Y., Liang, Y. P., Chang,

938   M., Liu, Y., and Lin, A. G.: Analysis of chemical characteristics of $PM_{2.5}$ in Beijing over a 1-year

939   period, J. Atmos. Chem., 73(4): 407-425, 2016c.

940   WHO. Health effects of black carbon. http://wedocs.unep.org/handle/20.500.11822/8699, 2012.

941   Wood, E. C., Canagaratna, M. R., Herndon, S. C., Onasch, T. B., Kolb, C. E., Worsnop, D. R., Kroll,

942   J. H., Knighton, W. B., Seila, R., Zavala, M., Molina, L. T., DeCarlo, P. F., Jimenez, J. L.,

943   Weinheimer, A. J., Knapp, D. J., Jobson, B. T., Stutz, J., Kuster, W. C., Williams, E. J.: Investigation

944   of the correlation between odd oxygen and secondary organic aerosol in Mexico City and Houston.

945   Atmos. Chem. Phys. 18(10), 8947-8968, 2010.

946   Wu, C., Wu, D., and Yu, J. Z.: Quantifying black carbon light absorption enhancement with a novel

947   statistical approach, Atmos. Chem. Phys., 18, 289-309, https://doi.org/10.5194/acp-18-289-2018,

948   2018.

949   Wu, D., Liao B. T, Wu M., Chen, H., Wang, Y., Niao, X., Gu, Y., Zhang, X., Zhao, X. J., Quan, J.

950   N., Liu, W. D., Meng, J., and Sun, D.: The long-term trend of haze and fog days and the surface

951   layer transport conditions under haze weather in North China, Acta Sci Circumst., 34, 1-11, 2014.

952 Wu, H., Zhang, Y. F., Han, S. Q., Wu, J. H., Bi, X. H., Shi, G. L., Wang, J., Yao, Q., Cai, Z. Y., Liu,

953 J. L., and Feng, Y. C.: Vertical characteristics of $PM_{2.5}$ during the heating season in Tianjin, China,

954 Sci. Total Environ., 523, 152-160, https://doi.org/10.1016/j.scitotenv.2015.03.119, 2015.

955 Wu, X., Wu, Y., Zhang, S., Liu, H., Fu, L., and Hao, J.: Assessment of vehicle emission programs

956 in China during 1998–2013: achievement, challenges and implications, Environ. Pollut., 214, 556-

957 567, 2016.

958 Xing, J., Wang, J., Mathur, R., Wang, S., Sarwar, G., Pleim, J., Hogrefe, C., Zhang, Y., Jiang, J.,

959 Wong, D. C., and Hao, J.: Impacts of aerosol direct effects on tropospheric ozone through changes

960 in atmospheric dynamics and photolysis rates, Atmos. Chem. Phys., 17, 9869-9883, 2017.

961 Xu, J., Wang, Q., Deng, C., McNeill, V. F., Fankhauser, A., Wang, F., Zheng, X., Shen, J., Huang,

962 K., and Zhuang, G.: Insights into the characteristics and sources of primary and secondary organic

963 carbon: High time resolution observation in urban Shanghai, Environ. Pollut., 233, 1177-1187,

964 https://doi.org/10.1016/j.envpol.2017.10.003, 2018.

965 Yang, F., He, K., Ye, B., Chen, X., Cha, L., Cadle, S.H., Chan, T., and Mulawa, P. A.: One-year

966 record of organic and elemental carbon in fine particles in downtown Beijing and Shanghai, Atmos.

967 Chem. Phys., 5, 1449–1457, 2005.

968 Yang, F., Huang, L., Duan, F., Zhang, W., He, K., Ma, Y., Brook, J. R., Tan, J., Zhao, Q., and Cheng,

969 Y.: Carbonaceous species in $PM_{2.5}$ at a pair of rural/urban sites in Beijing, 2005-2008, Atmos. Chem.

970 Phys., 11, 7893–7903, 2011a.

971 Yang, F., Tan, J., Zhao, Q., Du, Z., He, K., Ma, Y., Duan, F., and Chen, G.: Characteristics of $PM_{2.5}$

972 speciation in representative megacities and across China, Atmos. Chem. Phys., 11, 5207-5219,

973 2011b.

974 Yi, K., Liu, J. F., Wang, X. J., Ma, J. M., Hu, J. Y., Wan, Y., Xu, J. Y., Yang H. Z., Liu, H. Z.,

975 Xiang, S. L., and Tao, S.: A combined Arctic-tropical climate pattern controlling the inter-annual

976 climate variability of wintertime $PM_{2.5}$ over the North China Plain. Environ. Pollut., 245, 607-615,

977 2019.

978 Yu, X. Y., Cary, R. A., and Laulainen, N. S.: Primary and secondary organic carbon downwind of

979 Mexico City, Atmos. Chem. Phys., 9(18), 6793-6814, 2009.

980 Zhang, F., Zhao, J., Chen, J., Xu, Y., and Xu, L.: Pollution characteristics of organic and elemental

carbon in $PM_{2.5}$ in Xiamen, China, J. Environ. Sci., 23(8), 1342-1349, 2011.

Zhang, F., Wang, Z. W., Cheng, H. R., Lv, X. P., Gong, W., Wang, X. M., and Zhang, G.: Seasonal variations and chemical characteristics of $PM_{2.5}$ in Wuhan, central China, Sci. Total Environ., 518-519, 97-105, https://doi.org/10.1016/j.scitotenv.2015.02.054, 2015.

Zhang, R., Jing, J., Tao, J., Hsu, S. C., Wang, G., Cao, J., Lee, C. S. L., Zhu, L., Chen, Z., Zhao, Y., and Shen Z.: Chemical characterization and source apportionment of $PM_{2.5}$ in Beijing: seasonal perspective, Atmos. Chem. Phys., 13, 7053–7074, 2013.

Zhang, R. Y., Khalizov, A. F., Pagels, J., Zhang, D., Xue, H., and McMurry, P. H.: Variability in morphology, hygroscopicity, and optical properties of soot aerosols during atmospheric processing, Proc. Natl. Acad. Sci. U.S.A., 105, 10291–10296, 2008.

Zhang, Y., Li, C., Krotkov, N. A., Joiner, J., Fioletov, V., and McLinden, C.: Continuation of long-term global SO_2 pollution monitoring from OMI to OMPS, Atmos. Meas. Tech., 10, 1495-1509, https://doi.org/10.5194/amt-10-1495-2017, 2017.

Zhang, Y., Zhang, Q., Cheng, Y., Su, H., Li, H., Li, M., Zhang, X., Ding, A., and He, K.: Amplification of light absorption of black carbon associated with air pollution, Atmos. Chem. Phys., 18, 9879-9896, https://doi.org/10.5194/acp-18-9879-2018, 2018.

Zhao, M., Huang, Z., Qiao, T., Zhang, Y., Xiu, G., and Yu, J.: Chemical characterization, the transport pathways and potential sources of $PM_{2.5}$ in Shanghai: Seasonal variations, Atmos. Res., 158, 66-78, 2015a.

Zhao, M., Qiao, T., Huang, Z., Zhu, M., Xu, W., Xiu, G., Tao, J., and Lee, S.: Comparison of ionic and carbonaceous compositions of $PM_{2.5}$ in 2009 and 2012 in Shanghai, China, Sci. Total Environ., 536, 695-703, 2015b.

Zhao, P., Dong, F., and Yang, Y.: Characteristics of carbonaceous aerosol in the region of Beijing, Tianjin, and Hebei, China, Atmos. Environ., 71, 389-398, 2013.

Zheng, B., Tong, D., Li, M., Liu, F., Hong, C., Geng, G., Li, H. Y., Li, X., Peng, L. Q., Qi, J., Yan, L., Zhang, Y. X., Zhao, H. Y., Zheng, Y. X., He, K. B., and Zhang, Q.: Trends in China's anthropogenic emissions since 2010 as the consequence of clean air actions, Atmos. Chem. Phys., 18, 14095–14111, 2018.

Zhu, C., Tian, H., Hao, Y., Gao, J., Hao, J., Wang, Y., Hua, S., Wang, K., and Liu, H.: A high-resolution

1010   emission inventory of anthropogenic trace elements in Beijing-Tianjin-Hebei (BTH) region of China,

1011   Atmos. Environ., 191, 452-462, https://doi.org/10.1016/j.atmosenv.2018.08.035, 2018.
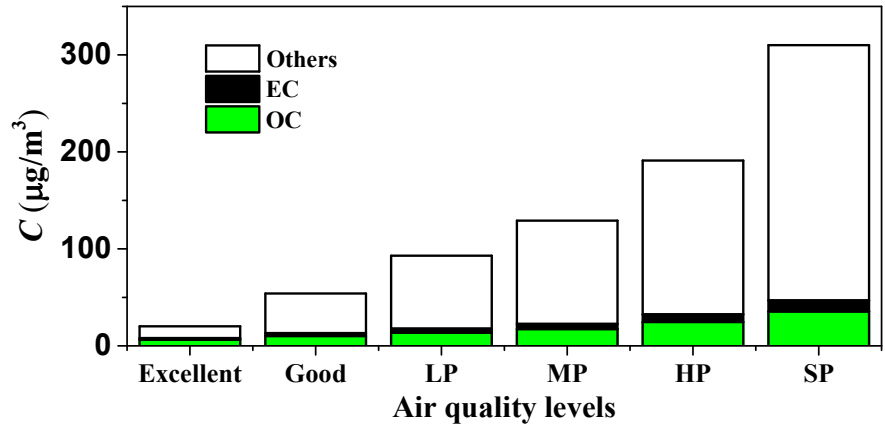
1012
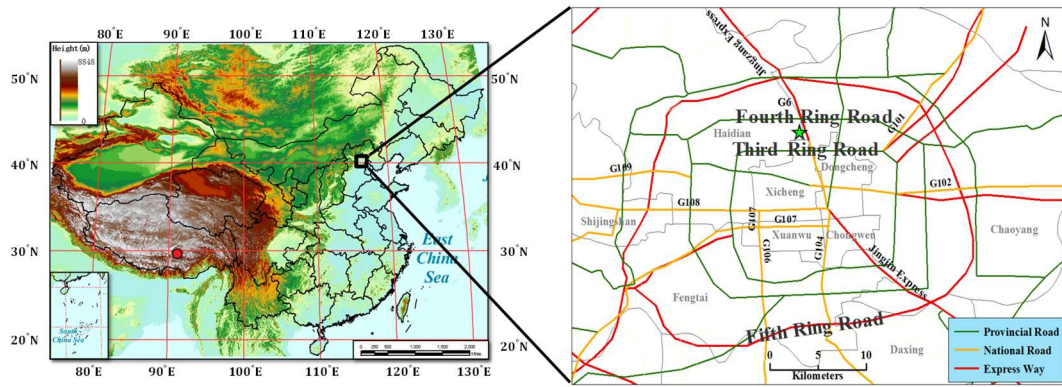
G6=Jingzang Expressway; G101=National Highway 101; G102= National Highway 102; G107= National Highway 107; G108= National Highway 108; G109= National Highway 109
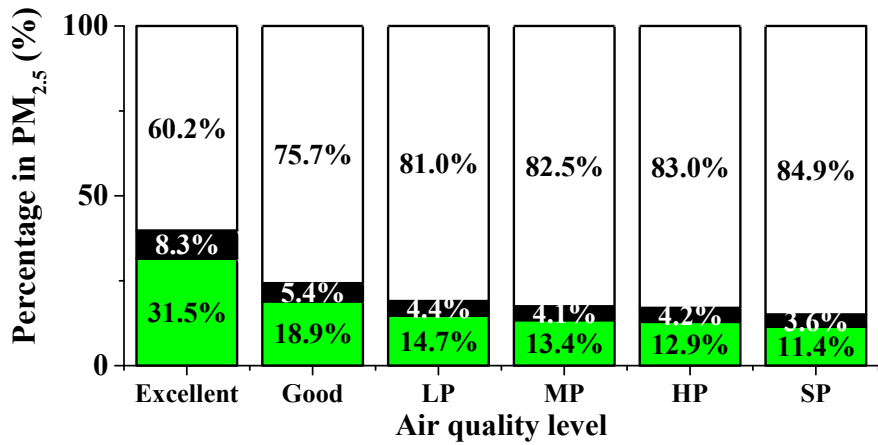
Fig. 1. Map with location of the sampling site (the asterisk in the right figure indicates the sampling site).
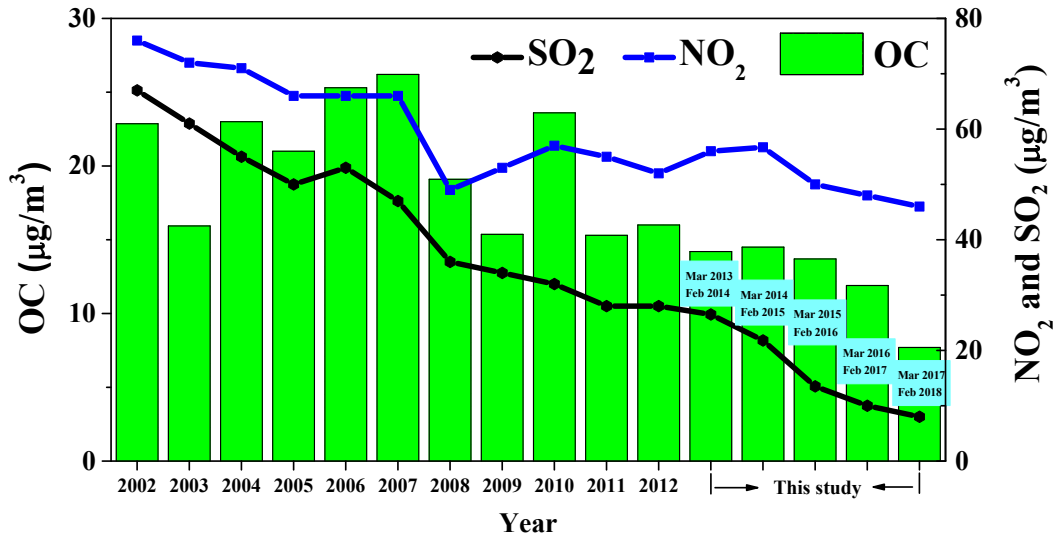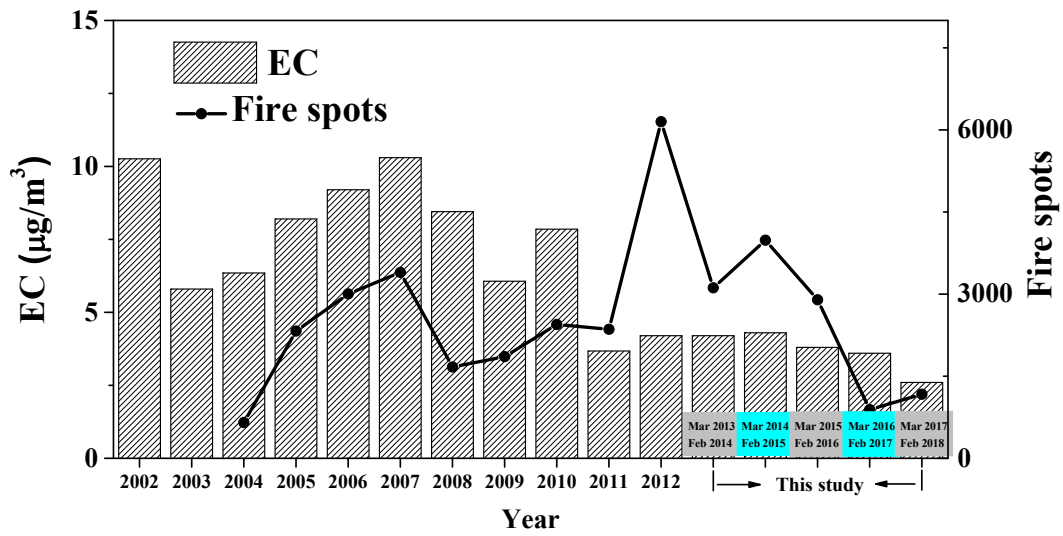
1017

1018

1019   Fig. 2. Variation of average OC, EC and $PM_{2.5}$ concentrations (top) and of the percentages of OC,

1020   EC and other components in $PM_{2.5}$ (bottom) for different air quality levels.

1021

1022

1023

Fig. 3. Variation of the annual mean OC and EC concentrations in $PM_{2.5}$ from 2002 to 2018 in Beijing. The variation in NO_2 and SO_2 concentrations and in the number of fire spots counted for the domain of (30-70° N, 65-150° E) is also shown.

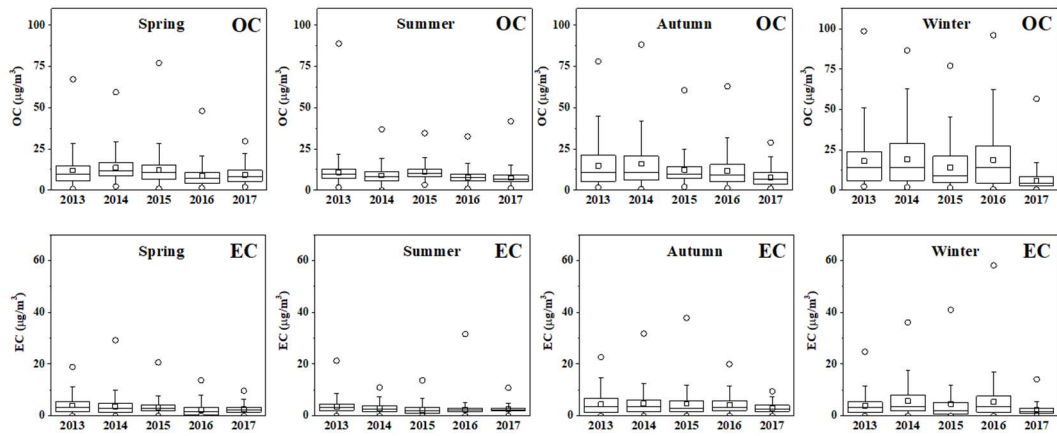1027

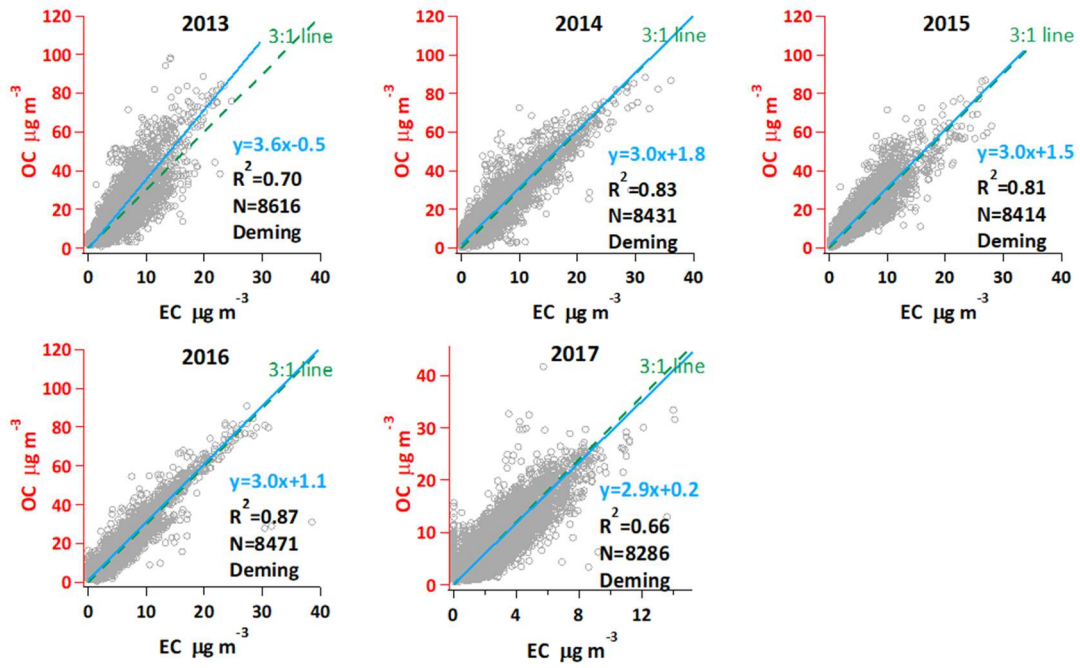1028

1029

1030

1031   Fig. 4. Seasonal variations of OC and EC concentrations from March 2013 to February 2018.

1032

1033

Fig. 5. Relationship between OC and EC using the Deming regression method from 2013 to 2017
(the dashed line indicates a OC/EC ratio of 3:1).

1036
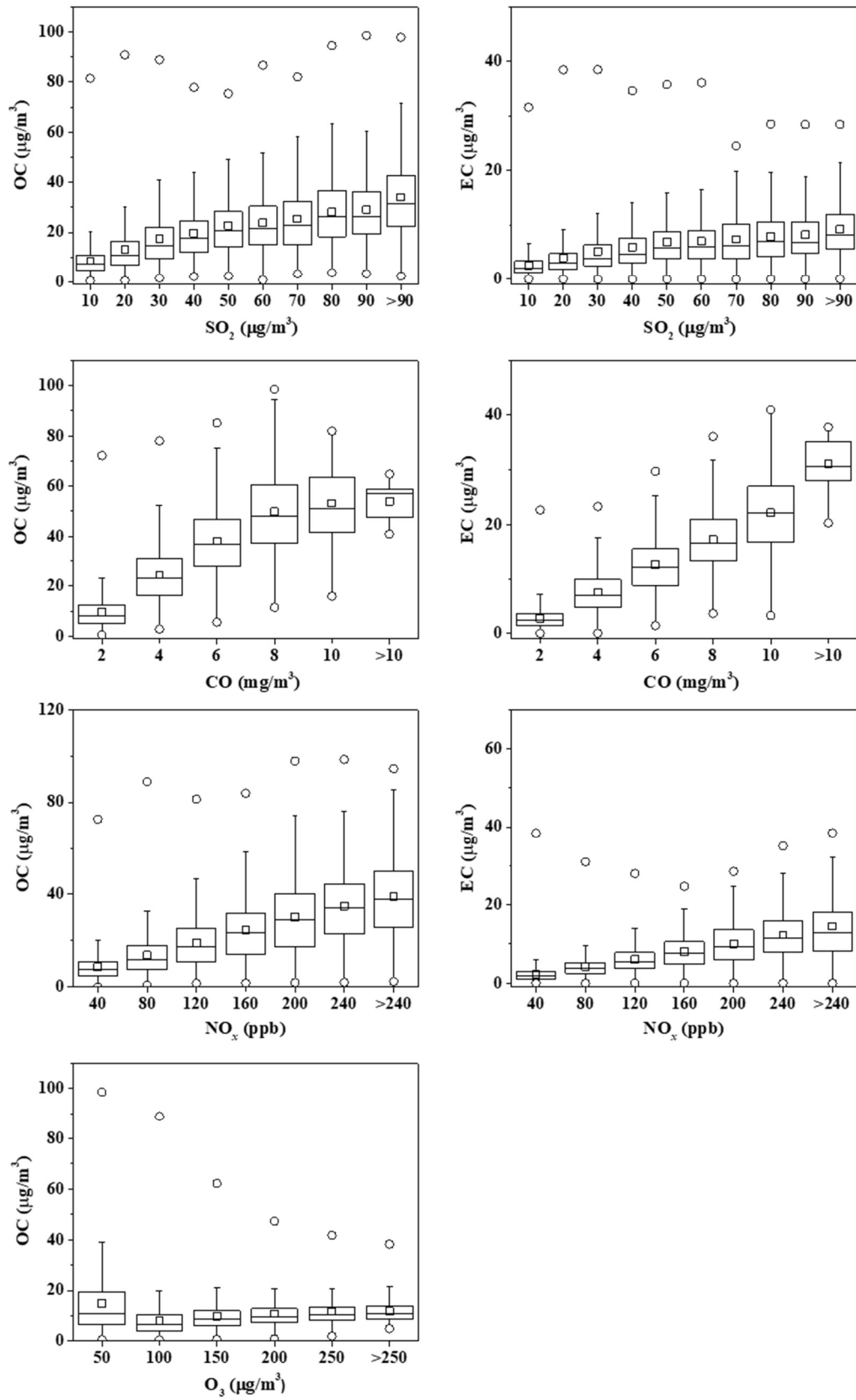
1037

1038   Fig. 6. OC and EC concentrations as a function of the SO_2, CO, NO_x and O_3 concentration.

1039

2013

2014

2015

2016
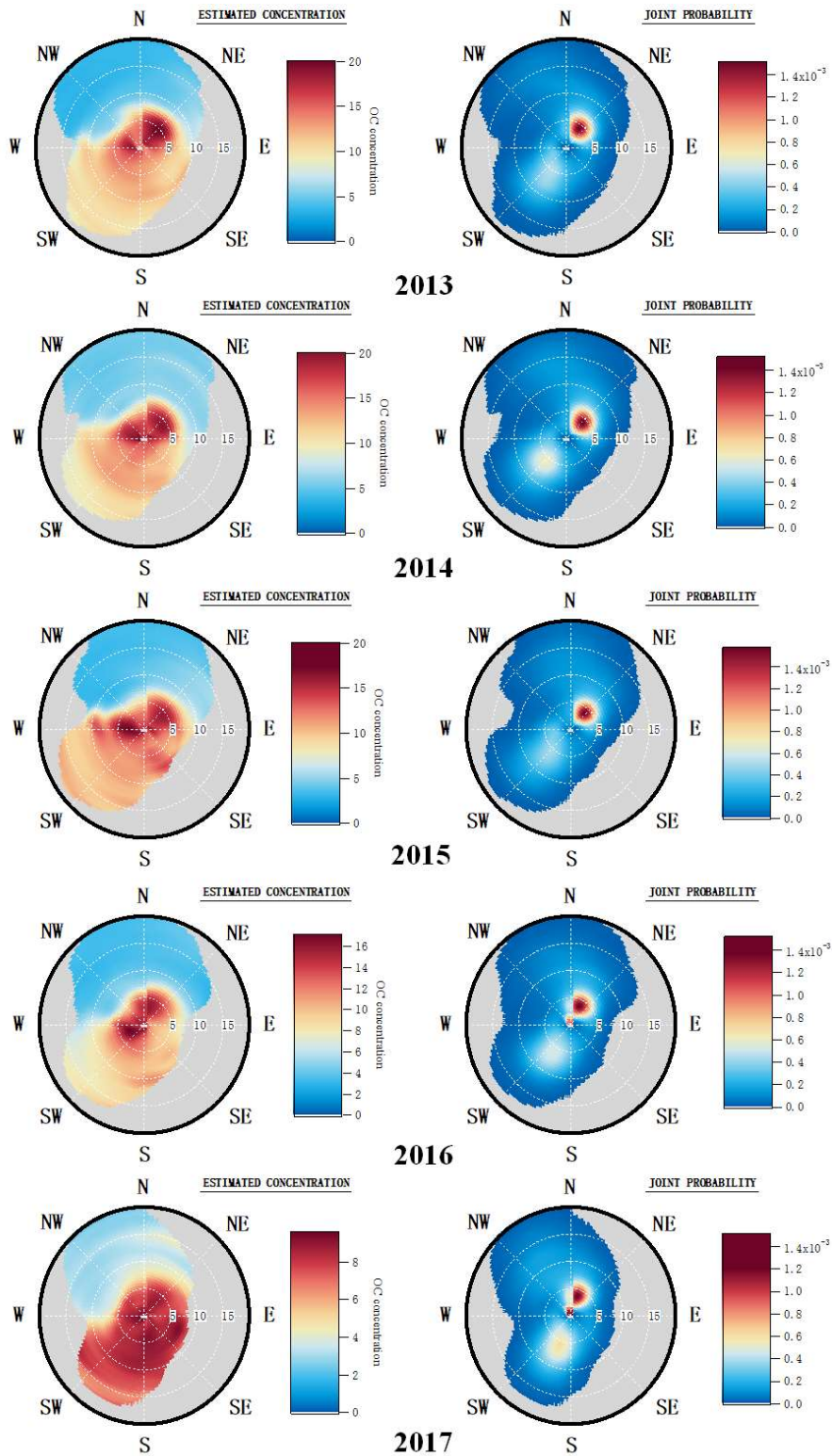
2017

1040

1041   Fig. 7. Wind analysis results using NWR on 1-h OC concentrations measured in Beijing from 2013
1042   to 2017 (Unit of wind speed: km/h).

1043
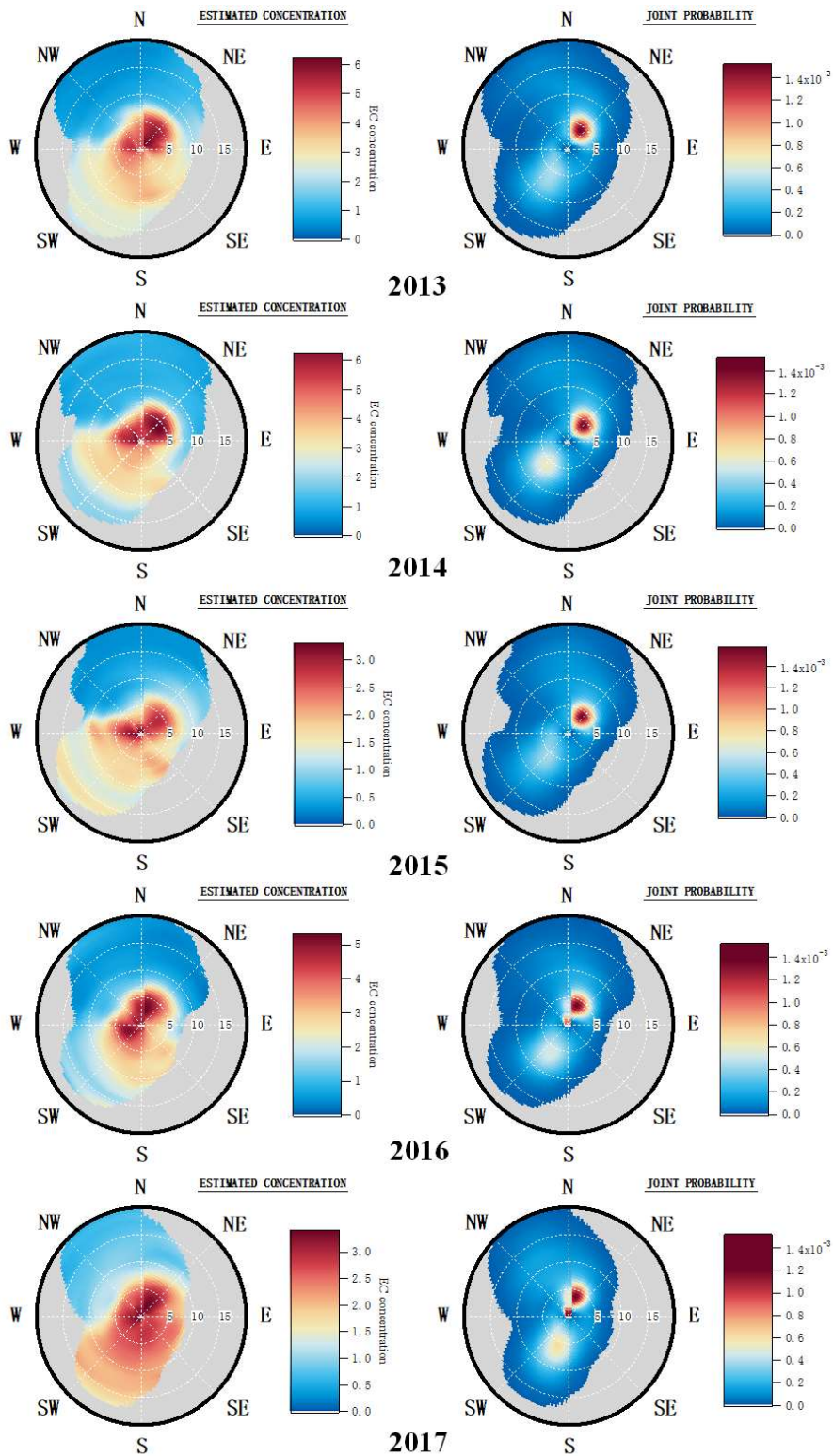
1044

Fig. 8. Wind analysis results using NWR on 1-h EC concentrations measured in Beijing from 2013
to 2017.

1047

Fig. 9 Potential source areas for OC and EC in Beijing from 2013 to 2017. The color code denotes the PSCF probability. The measurement site is indicated with a ⦿. The identification of the provinces is given in Fig. S9.

1053 Table 1. Medians, averages and associated standard deviations for the OC, EC and PM2.5 concentrations (in µg/m^3) and averages for the OC/PM$_{2.5}$, EC/PM$_{2.5}$ and
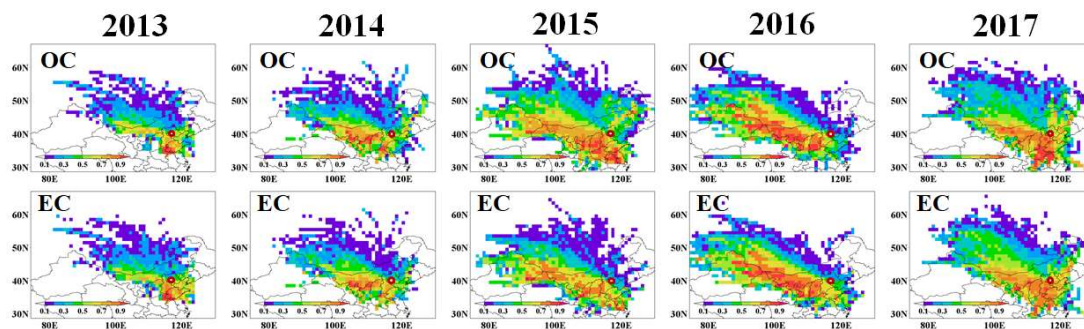
1054 TC/PM$_{2.5}$ ratios from March 2013 to February 2018.

	OC			EC			PM$_{2.5}$			OC/PM$_{2.5}$	EC/PM$_{2.5}$	TC/PM$_{2.5}$
	Median	Average	Stdev	Median	Average	Stdev	Median	Average	Stdev	Average	Average	Average
Mar-2013 − Feb-2014	10.6	14	11.7	3.2	4	3.3	66	89	82.9	0.157	0.045	0.203
Mar-2014 − Feb-2015	10.4	14.5	12.1	3	4.3	4	66	85.5	76.6	0.169	0.05	0.219
Mar-2015 − Feb-2016	9.1	13.7	9.2	1.3	3.8	4.4	48	76.9	85.6	0.178	0.049	0.228
Mar-2016 − Feb-2017	8.2	11.9	11.3	2.5	3.6	3.7	53	79.4	82.8	0.15	0.045	0.195
Mar-2017 − Feb-2018	6.8	7.7	4.7	2.3	2.6	1.6	35	49.4	48.6	0.155	0.052	0.208
whole study period	9.3	12.4	10.6	2.7	3.7	3.6	52	75.7	77.6	0.164	0.049	0.213

1055

1056 Table 2. Mean or median OC and EC mass concentrations (in μg/m^3) observed in major megacities of the world published in the literature and obtained in this study.

1057

1058

Megacities	Method	Period	Number or frequency of sampling	OC	EC	Literature
Athens	TOT	May 2008 to April 2013	Once everyday	2.1	0.54	Paraskevopoulou et al., 2014
Beijing	TOT	March 2017-Feburary 2018	Hourly	7.7	2.6	This study
Hongkong	TOR	from July to October 2014 and December 2014 to March 2015	N=161	7.8	2.2	Chen et al., 2018
Lhasa	TOR	May 2013 to March 2014	once each week	3.27	2.24	Li et al., 2016
Los Angele	TOT	March 2017-Feburary 2018	once every 3 days	2.88	0.56	US EPA*
Mexico	TOT	March 2006	Hourly	5.4-6.4	0.6-2.1	Yu et al., 2009
Mumbai	TOT	March-May 2007, October-November 2007 and December-January 2007-2008	15 days in a season	20.4-31.3	5.0-9.2	Villalobos et al., 2015
New Delhi	TOR	January 2013 -May 2014	N=95	17.7	10.3	Sharma and Mandal, 2017
New York	TOT	March 2017-Feburary 2018	Once every 3 days	2.88	0.63	US EPA*
Paris	TOT	from 11 September 2009 to 10 September 2010	Once everyday	3.0	1.4	Bressi et al., 2013
São Paulo	TOT	2014	Once each Tuesday	10.2	7	Pereira et al., 2017
Shanghai	TOT	from July 2013 to June 2014	Hourly	8.4	3.1	Xu et al., 2018
Soul	TOT	from January 2014 to December 2014	Hourly	4.1	1.6	Park et al., 2015
Tianjin	TOR	from Dec 23, 2013, to Jan 16, 2014	N=25	30.53	8.21	Wu et al., 2015
Tokyo	TOT	from July 27 to August 15, 2014	Once everyday	2.2	0.6	Miyakawa et al., 2016
Toronto	TOT	December 1, 2010-November 30, 2011	Hourly	3.39	0.5	Sofowote et al., 2014
Wuhan	TOT	From August 2012 to July 2013	Once every six days	16.9	2.0	Zhang et al., 2015
Xi'an	TOR	Four months of 2010	N=56	18.6	6.7	Wang et al., 2015

1059 *https://aqs.epa.gov/api

1060 TOR: thermal-optical reflectance; TOT: thermal-optical transmittance

1061   Table 3. OC/EC ratios in main domestic and foreign cities.

	Cities	Period	Method	OC/EC	References
		1999-2000	TOR	2.7	He et al., 2001
		2000	TOT	7.0	Song et al., 2006
		2001-2002	EA	2.6	Duan et al., 2006
		2005-2006	TOT	3.0	Yang et al., 2011b
		2008	TOT	2.2	Yang et al., 2011a
		2008-2010	TOR	4.4	Hu et al., 2015
Domestic cities	Beijing	2009-2010	TOR	2.9	Zhao et al., 2013
		2009-2010	TOT	3.4	Zhang et al., 2013
		2012-2013	TOT	7.0	Wang et al., 2016c
		2013	TOT	5.0	Ji et al., 2018
		2014	TOT	4.8	Ji et al., 2018
		2013	TOT	3.6	This study
		2014	TOT	3.0	This study

49

	2015	TOT	3.0	This study
	2016	TOT	3.0	This study
	2017	TOT	2.9	This study
Baoji	March 2012 - March 2013	TOR	5.3	Niu et al., 2016
Chengdu	2009-2010 annual	TOR	2.5	Tao et al., 2013
	2009–2013	TOR	4.4	Shi et al., 2016
	2011 annual	TOR	2.4	Tao et al., 2014
	2012-2013 annual	TOT	4.1	Chen et al., 2014
Chongqing	2005-2006 annual	TOR	4.7	Yang et al., 2011b
	2012-2013 annual	TOT	3.8	Chen et al., 2014
	May 2012-May 2013	TOT	3.6	Chen Y. et al., 2017
Ya'an	June 2013 - June 2014	TOT	13.3	Li et al., 2018
Hangzhou	2004-2005 annual	EA	2.0	Liu G. et al., 2015
Hongkong	July - October 2014 and December 2014 - March 2015	TOR	3.5	Chen et al., 2018
Lhasa	May 2013 - March 2014	TOR	1.5	Li et al., 2016

Nanjing	2014 annual	TOT	1.8	Chen D. et al., 2017
	2011-2014 annual	TOR	2.6	Li et al., 2015
Ningbo	2009-2010 annual	TOR	2.8	Liu et al., 2013
Neijiang	2012-2013 annual	TOT	4.5	Chen et al., 2014
Qingling	March 2012 - March 2013	TOR	6.3	Niu et al., 2016
Shanghai	2009 annual	TOR	3.4	Zhao et al., 2015a
	2011	TOT	2.6	Chang et al., 2017
	2012	TOT	2.9	Chang et al., 2017
	2012 annual	TOR	5.4	Zhao et al., 2015b
	2013	TOT	3.4	Chang et al., 2017
Shijiazhuang	Four seasons (2009-2010)	TOR	2.7	Zhao et al., 2013
Tianjin	2009-2010	TOR	2.7	Zhao et al., 2013
Xi'an	2010 annual	TOR	2.7	Wang et al., 2015
	March 2012 - March 2013	TOR	4.0	Niu et al., 2016
	March 2012 - March 2013	TOR	4.0	Niu et al., 2016

		March 2012 - March 2013	TOR	3.8	Niu et al., 2016
		December 2014 - November 2015	TOT	10.4	Dai et al., 2018
	Weinan	March 2012 - March 2013	TOR	4.4	Niu et al., 2016
	Wuhan	From August 2012 - July 2013	TOT	8.5	Zhang et al., 2015
Foreign cities	Athens	May 2008 - April 2013	TOT	3.9	Paraskevopoulou et al. 2014
	Los Angeles	March 2017-Feburary 2018	TOT	5.1	US EPA*
	New Delhi	January 2013 -May 2014	TOR	1.7	Sharma and Mandal, 2017
	New York	March 2017-Feburary 2018	TOT	4.6	US EPA*
	Paris	September 11, 2009 - September 10, 2010	TOT	2.1	Bressi et al., 2013
	São Paulo	2014	TOT	1.5	Pereira et al., 2017
	Seoul	January 2014 - December 2014	TOT	2.6	Park et al., 2015
	Tokyo	July 27 - August 15, 2014	TOT	3.7	Miyakawa et al., 2016
	Toronto	December 1, 2010-November 30, 2011	TOT	6.8	Sofowote et al., 2014

1062   *https://aqs.epa.gov/api

1063   TOR: thermal-optical reflectance; TOT: thermal-optical transmittance; EA: elemental analysis